Title:

Small RNA-mediated genomic silencing promotes telomere stability in the absence of telomerase in *C. elegans*

Authors:

Charlie Longtine[1,2,#], Stephen Frenk[1,2,#], Evan H. Lister-Shimauchi[1,2], and Shawn Ahmed[1,2,3*]

Affiliations:

[1]Department of Genetics, [2]Department of Biology, [3]Lineberger Comprehensive Cancer Center, University of North Carolina, Chapel Hill, NC, USA

# Equal contributions
*Correspondence: shawn@med.unc.edu

Running title: small RNAs promote telomere stability

Keywords: telomere, telomerase, siRNA, sRNA, RNA interference

Abstract

We define an endogenous small RNA pathway in *Caenorhabditis elegans* that protects telomeres via Dicer, the perinuclear Argonaute protein WAGO-1, the nuclear Argonaute protein HRDE-1, and the HP1 protein HPL-2 that stabilizes the heterochromatin mark H3K9me2. Loss of telomerase induces biogenesis of subtelomeric small RNAs, whereas loss of both telomerase and small RNA-mediated genome silencing induces expression of the telomeric lncRNA TERRA, DNA damage, and accelerated sterility. These phenotypes were rescued by exogenous telomeric small RNAs and by loss of the DNA damage response protein EXO-1. Although ATRX promotes heterochromatin deposition and is lost in human tumors that maintain their telomeres via ALT, we detected only a modest role for the *C. elegans* ATRX ortholog XNP-1 in telomere protection in the absence of telomerase. Moreover, neither XNP-1 nor small RNA factors that promote telomere stability in the absence of telomerase repress ALT in *C. elegans*. We propose that small RNA-mediated heterochromatin formation and telomerase function redundantly to repress a form of telomeric DNA damage that induces TERRA expression. We conclude that small RNA-mediated genome silencing promotes telomere stability in the absence of telomerase.

Article Summary

We found that a number of small RNA biogenesis factors and heterochromatin proteins promoted telomere stability in the absence of telomerase. The telomeric non-coding RNA TERRA and DNA damage signaling were induced upon loss of small RNAs and telomerase, indicating that small RNAs directly or indirectly repress TERRA expression and telomeric DNA damage, both of which were suppressed when telomerase acts to heal telomeric damage. These findings reveal a functional interaction between small RNAs and telomere biology that is relevant to the fields of aging, genome stability and small RNAs.

Introduction

Telomeres are repetitive nucleoprotein structures that protect the ends of linear eukaryotic chromosomes from degradation and recognition as double-stranded DNA breaks (Maciejowski and de Lange, 2017, Shay, 2016). Deficiency for telomerase reverse transcriptase in most human somatic cells results in progressive telomere erosion over cell divisions, which eventually triggers replicative senescence (Holohan et al., 2014, Shay, 2016). This telomere clock acts as a barrier to tumorigenesis, but may also contribute to organismal aging through impaired stem cell function, regeneration, and organ maintenance (Donate and Blasco, 2011, Shay, 2016). Regulating the rate of telomere erosion in telomerase-negative cells is therefore crucial for maintaining the balance between tumor suppression and age-related tissue decline (Li et al., 2017, Maciejowski and de Lange, 2017). Tumor cells escape telomere-triggered senescence by stabilizing telomere length, either through reactivation of telomerase or through activation of the telomerase-independent recombination-mediated telomere maintenance pathway termed Alternative Lengthening of Telomeres (ALT) (Pickett and Reddel, 2015).

Telomeres have features characteristic of heterochromatin in that they associate with the heterochromatin protein HP1 and contain transcriptionally repressive histone marks such as methylation of H3K9 and H4K20 (Benetti et al., 2007, McMurchy et al., 2017). Nonetheless, telomeres are transcribed into the G-rich long noncoding RNA (lncRNA) termed TERRA, a feature widely conserved among eukaryotes (Azzalin et al., 2007). TERRA is transcribed from the subtelomere into the telomere by RNA polymerase II and is upregulated at shortened and damaged telomeres, where it may recruit telomerase and chromatin modifiers to promote telomere elongation (Azzalin and Lingner, 2015, Cusanelli et al., 2013). Telomere elongation represses expression of TERRA through increased heterochromatin marks at telomeres such as histone H3K9 methylation and HP1 binding (Arnoult et al., 2012). In contrast, shortened telomeres of mice deficient for telomerase or of mouse cells that overexpress the telomere-binding protein TRF2 display loss of heterochromatic marks at telomeres and subtelomeres (Benetti et al., 2007, Benetti et al., 2008). Telomere length has therefore been inversely correlated with TERRA expression and the heterochromatic state of telomeres, and

101 TERRA expression in mouse cells has recently been linked to H3K9me3 and other
102 heterochromatic histone marks present at mammalian telomeres (Montero et al., 2018).
103
104 Transcriptional silencing and heterochromatin deposition at repetitive segments of the
105 genome such as the pericentromere require long non-coding RNA (lncRNA) transcripts
106 that promote biogenesis of and interact with small RNAs (sRNAs) that direct
107 heterochromatin factors to target these genomic loci (Holoch and Moazed, 2015,
108 Reinhart and Bartel, 2002). Endogenous sources of double-stranded RNA such as
109 sense-antisense transcript hybrids can be processed into small RNAs that play roles in
110 creating and maintaining sRNA-mediated heterochromatin. In this context, RNA
111 expression is paradoxically required for genomic silencing (Holoch and Moazed, 2015).
112 Bidirectional transcription of telomeres has been linked to production of telomeric
113 sRNAs that are associated with the presence of subtelomeric DNA methylation in
114 *Arabidopsis* (Vrbsky et al., 2010). Similar telomeric sRNAs have also been observed in
115 *Tetrahymena*, mouse stem cells, and human cell lines (Cao et al., 2009, Couvillion et
116 al., 2009, Rossiello et al., 2017), and can promote the DNA damage response at
117 uncapped telomeres in mammals (Cao et al., 2009, Couvillion et al., 2009, Rossiello et
118 al., 2017). However, their functional relevance at canonical telomeres and their
119 interaction with telomerase is not well understood.
120
121 Germline transcription in *C. elegans* is regulated in part by a network of small RNA
122 pathways that promote silencing or expression of target loci in a sequence-specific
123 manner (Billi et al., 2014). Primary sRNA classes trigger production of secondary
124 sRNAs that can promote transcriptional silencing or mRNA destruction. One class of
125 primary sRNAs are 21 nucleotide Piwi-Interacting RNAs (piRNAs) that are created from
126 thousands of tiny genes that repress expression of potentially harmful foreign genetic
127 elements including transposons and transgenes (Batista et al., 2008, Das et al., 2008,
128 Kasper et al., 2014). piRNAs interact with PRG-1, a member of the Piwi clade of
129 Argonaute proteins, which can recognize piRNA targets based on sequence
130 complementarity with up to 3 mismatches (Bagijn et al., 2012). RNA target recognition
131 triggers the recruitment of RNA-dependent RNA polymerases (RdRPs) that act in

132 Mutator bodies, which are associated with perinuclear P granules, to create *de novo* 22
133 nucleotide secondary sRNAs with a 5' guanine (22G RNAs) (Pak and Fire, 2007).
134 These 22G RNAs are loaded onto worm-specific Argonaute proteins (WAGOs) such as
135 the nuclear WAGO HRDE-1, which promotes heterochromatin deposition at target loci
136 (Ashe et al., 2012, Buckley et al., 2012). Germline transcription is protected by a
137 separate set of 22G RNAs that interact with the anti-silencing Argonaute protein CSR-1
138 (Avgousti et al., 2012, Wedeles et al., 2013). Aside from the piRNA pathway, 22G RNAs
139 can be created in response to primary sRNAs derived from other sources. For example,
140 DCR-1, the *C. elegans* homologue of the highly conserved RNAse class III enzyme
141 Dicer, can cleave endogenous double stranded RNA to create primary 26G RNAs,
142 which bind distinct Argonaute proteins to trigger RDRP-dependent silencing through the
143 22G RNA pathway described above (Bernstein et al., 2001, Ketting et al., 2001, Knight
144 and Bass, 2001).
145
146 Here we describe an endogenous sRNA and heterochromatin pathway that functions
147 redundantly with telomerase to repress TERRA and promote telomere stability.
148
149
150 **Materials and Methods**
151
152 Strains: Unless otherwise noted, all strains were maintained at 20°C on nematode
153 growth medium plates seeded with *Escherichia coli* OP50. Strains used include Bristol
154 N2 ancestral, *wago-1(tm1414)*, *trt-1(ok410), unc-29(e193), dpy-5(e61), dcr-1(mg375),*
155 *hrde-1(tm1200), rde-1(ne219), rde-4(ne299), rrf-3(mg373), rrf-2(ok210), eri-1(mg366),*
156 *mut-7(pk204), mut-7(pk720), mut-14(pk738), rbr-2(tm1231), spr-5(by101), xnp-*
157 *1(ok1823), xnp-1(tm678), hpl-1(tm1624), hpl-2(ok916), hpl-2(tm1479),* and *exo-*
158 *1(tm1842)*. A *trt-1 unc-29* double mutant, where *unc-29* is tightly linked to *trt-1*, was
159 used to create strains used in this study. Double, triple, and quadruple mutants were
160 created using standard marker mutations and verified based on phenotype or genotype.
161 *mut-7* and *mut-14* mutants are known to accumulate transposon-induced mutations, so
162 these strains were outcrossed several times before use.

163 DAPI staining: One-day-old adults were washed twice in M9, soaked in 150 µL of
164 400ng/mL DAPI in ethanol solution for 30 min or until evaporated, rehydrated in 2 mL of
165 M9 solution overnight at 4°C, and mounted in 8 µL VECTASHIELD mounting medium
166 (Vector Laboratories). Chromosome counts were performed under 60x magnification
167 and a 359nm excitation wavelength using a Nikon Eclipse E800 microscope.

168 qPCR: Non-starved mixed-stage worms were washed with M9 and RNA was extracted
169 using 1 mL TRIZOL according to the manufacturer's instructions. For RT-PCR analysis,
170 total RNA was treated twice with DNase I and was reverse transcribed with primers for
171 a reference gene *act-1* and a telomere-specific primer $(GCCTAA)_3$ using SuperScript II
172 reverse transcriptase (Invitrogen). For SYBR green reactions, subtelomere specific
173 primers were designed within 200bp of the telomere-subtelomere junction.
174
175 RNA FISH: RNA FISH was performed as previously described (Sakaguchi et al., 2014)
176 with several modifications. In brief, non-starved, mixed-stage animals were washed
177 twice in M9 and three times in 1x DEPC-treated PBS. Worms were fixed in 1mL fixation
178 buffer (1x DEPC-treated PBS with 3.7% formaldehyde) for 45 min rotating at room
179 temperature then washed twice in 1mL 1x DEPC-treated PBS. Fixed animals were
180 permeabilized overnight at 4°C in 70% ethanol in DEPC-treated H_2O, then washed in 1
181 mL wash buffer [10% (vol/vol) formamide in 2x RNases-free SSC]. Aliquots of each
182 sample were removed prior to hybridization and treated with RNaseA for 1h at 37°C to
183 ensure probe specificity to RNA. Hybridization was performed at 30°C overnight in 100
184 µL hybridization buffer (10% dextran sulfate, 2x RNase-free SSC, 10% deionized
185 formamide, 0.02% RNase-free BSA, 50 µg *E. coli* tRNA) with 1.25 µM probe. Cy5-
186 labelled $(GCCTAA)_3$ probe was used to detect TERRA transcripts. Animals were
187 washed twice with wash buffer, counterstained with 25 ng/mL DAPI for 30 min at room
188 temperature, and mounted on glass slides in VECTASHIELD mounting medium (Vector
189 Laboratories) before epifluorescence microscopy.
190
191 IF: IF was carried out as previously described (Phillips et al., 2009) by fixing dissected
192 gonads of 1 day old adults in 2% PFA for 10 minutes followed by a 1 minute postfixation
193 in methanol. Rabbit anti-pS/TQ (Cell Signaling Technology) was used at a 1:500 dilution

194 and mouse anti-RNA:DNA hybrid S9.6 at 1:500 dilution. Stained gonads were
195 counterstained with DAPI and mounted with VECTASHIELD (Vector laboratories)
196 before epifluorescence microscopy.
197
198 RNAi: RNAi clone expressing dsRNA targeting *C. elegans* telomeres was constructed
199 using NEB HiFi DNA assembly mix according to the manufacturer's instructions. 200
200 bp of telomeric repeats were amplified from cTel55x by PCR with 20 bp overlap to SpeI
201 digested L4440. Correct constructs were transformed into HT115 and RNAi was
202 performed as previously described (McMurchy et al., 2017).
203
204 Southern Blot: *C. elegans* genomic DNA was digested overnight with Hinf1 (New
205 England Biolabs), separated on a 0.8% agarose gel at 1.5 V/cm, and transferred to a
206 neutral nylon membrane (Hybond-N, GE Healthcare Life Sciences). A digoxigenin-
207 labelled telomere probe was hybridized and detected as described (Ahmed and
208 Hodgkin, 2000). Migration distance was measured using ImageJ.
209
210 Mrt and ALT assays: When telomerase-deficient *trt-1(ok410) C. elegans* mutants are
211 passaged by using the standard Mortal Germline (Mrt) assay developed in our
212 laboratory, which involves passaging six L1 larval animals to fresh plates weekly, 100%
213 become sterile within 20–30 generations. When *trt-1(ok410)* strains are passaged
214 weekly by transferring a 1cm^2 chunk of agar populated with ≈200–400 animals, 10-20%
215 of the strains survive for hundreds of generations. Mantel-Cox Log Rank Analysis was
216 used to determine differences of transgenerational lifespan between strains. A z-test
217 was performed to compare proportion of ALT survivors in chunked strains.
218
219 RNA-seq: Animals were grown at 20°C on 100 mm NGM plates seeded with OP50
220 bacteria. Two biological replicates were prepared for each genotype. RNA was
221 extracted using Trizol (Ambion) followed by isopropanol precipitation. RNA samples
222 were treated with 20U RNA 5' polyphosphatase (Lucigen, RP8092H) for 30 minutes at
223 37°C to remove 5' triphosphate groups. Library preparation and sequencing was
224 performed at the UNC School of Medicine High-Throughput Sequencing Facility

225 (HTSF). RNA-seq libraries were prepared using the NEXTflex Small RNA Library Prep
226 Kit for Illumina (Bio Scientific). Libraries were sequenced on an Illumina HiSeq 2500 to
227 produce approximately twenty million 50 bp single-end reads per library.
228
229 Analysis of high throughput sequencing data: Adapter trimming was performed as
230 required using the bbduk.sh script from the bbmap suite3 and custom scripts (Bushnell,
231 2016). Reads were then filtered for 22G species or all species between 18 and 30
232 nucleotides in length using a custom python script. Reads were then converted to fasta
233 format and mapped to the *C. elegans* genome (WS251) using bowtie (Langmead et al.,
234 2009) with the following options: -M 1 -v 0 -best -strata. Uniquely mapping sRNAs were
235 detected by replacing the -M 1 parameter with -m 1. To detect telomere-mapping
236 sRNAs, reads were mapped to seven repeats of perfect telomere sequence (TTAGGC),
237 allowing for zero mismatches. Unmapped reads were re-mapped to the telomere
238 sequence, this time allowing for one mismatch. This step was repeated to detect reads
239 that map to telomeres with two or three mismatches. Genes with differential sRNA
240 abundance in *trt-1* were identified using DESeq2 (Love et al., 2014). To detect changes
241 in the abundance of subtelomeric sRNAs in *trt-1* and *trt-1; dcr-1*, 22G reads mapping to
242 the 2kb of sequence adjacent to the telomere were counted for each chromosome arm.
243 Counts were normalized by dividing by the total number of mapped reads for each
244 library. A pseudocount of 1 was added to each normalized value to avoid division by
245 zero errors. Replicates were averaged and the log2-fold change between mutant and
246 wildtype was calculated for each subtelomere. Analysis of sequencing data was
247 performed using the R statistical computing environment (Team, 2017). Genome
248 regions were visualized using the Gviz R package (Hahne and Ivanek, 2016).
249 Immunoprecipitation datasets were used in Figure 3G, H but were excluded from the
250 analysis shown in Figure 3D-F. To detect sRNAs targeting transposons, 22G reads
251 were mapped to the *C. elegans* transposon consensus sequences downloaded from
252 Repbase with bowtie, allowing for up to two mismatches. ChIP-seq reads were mapped
253 to the genome as fastq files as described above without the size-filtering step. Read
254 coverage was calculated at each base using bedtools (Quinlan and Hall, 2010).
255 Coverage values were normalized by dividing by the number of total mapped reads for

256 each library and enrichment was calculated by dividing the normalized coverage for IP
257 libraries by the normalized coverage of their respective input libraries.
258
259
260 **Results**
261
262 **Loss of endogenous sRNAs or XNP-1/ATRX does not promote ALT**
263 High levels of TERRA and loss of the histone H3.3 chaperone subunits ATRX and
264 DAXX commonly occur in human ALT cancers (Flynn et al., 2015, Lovejoy et al., 2012).
265 The ATRX/DAXX complex mediates histone H3.3 incorporation at telomeres and
266 interacts with methylated H3K9 and HP1 to promote heterochromatin formation (Wong
267 et al., 2010), which has been proposed to repress ALT by protecting telomeres from
268 replication stress and TERRA expression (Udugama et al., 2015). We have previously
269 shown that 10-20% of *C. elegans* strains that are deficient for telomerase can be
270 maintained indefinitely through the activation of ALT (Cheng et al., 2012). Because
271 human ALT cancers are characterized by ATRX-mediated heterochromatin dysfunction,
272 we reasoned that small RNA factors that promote heterochromatin silencing might
273 regulate the establishment of ALT. We tested this hypothesis by passaging *trt-1*
274 telomerase mutant strains that were deficient for biogenesis of either primary or
275 secondary sRNAs by transferring hundreds of worms per strain weekly, which reliably
276 allows survival of 10-20% of strains via ALT (Cheng et al., 2012). Loss of either primary
277 sRNAs (*trt-1; dcr-1)* or downstream secondary sRNAs (*trt-1; mut-7* and *trt-1; mut-14)* did
278 not significantly alter the proportion of strains that survive via ALT (Figure 1A, Table
279 S1). Similarly, loss of the histone H3.3 chaperone XNP-1/ATRX itself did not affect the
280 establishment or maintenance of ALT (Table S1), indicating that loss of neither sRNA-
281 nor XNP-1/ATRX-mediated heterochromatin formation is sufficient to promote ALT in *C.*
282 *elegans*.
283
284 **Small RNA and heterochromatin factors repress rapid sterility when telomerase is**
285 **deficient**

286 *C. elegans trt-1* telomerase mutant strains do not remain fertile via ALT when 6 worms
287 are passaged weekly. Instead, when 20-40 strains per genotype are passaged,
288 telomere erosion and chromosome fusion results in uniform sterility after growth for 20-
289 30 generations (Ahmed and Hodgkin, 2000, Cheng et al., 2012, Meier et al., 2006). The
290 sterility of late-generation *trt-1* mutants is analogous to crisis observed in checkpoint-
291 deficient telomerase-negative mammalian cells. Intriguingly, *trt-1* mutant lines lacking
292 primary or secondary sRNA biogenesis factors became sterile significantly faster than
293 *trt-1* single mutants when they were passaged by transferring 6 L1 larvae per week
294 (Figure 1B, Table S2). sRNA-deficient *trt-1* mutant strains rapidly accumulated end-to-
295 end chromosome fusions by generation F12, a characteristic of telomerase mutants that
296 have grown for more than 20 generations (Figure 1G). *C. elegans* chromosome fusions
297 cause non-disjunction events during meiosis that elicit dominant embryonic lethality or
298 X0 male phenotypes in progeny of heterozygous F1 animals. We asked if early-
299 generation *trt-1; dcr-1* mutant animals possessed chromosome fusions by performing
300 genetic crosses that would be capable of revealing a single heterozygous end-to-end
301 chromosome fusion (Ahmed and Hodgkin, 2000). We crossed four independently
302 derived *trt-1 dcr-1* F4 hermaphrodites with N2 wild-type males but failed to detect fused
303 chromosomes that were present in generation F24 *trt-1* mutant controls ($p = 3.841e-05$
304 for males and $p = 3.61e-05$ for dead embryos, Mann Whitney U test) (Table S3).
305 However, early-generation *trt-1; dcr-1* mutant strains displayed high levels of DNA
306 damage that were not observed for *trt-1* single mutant controls (Figure 1H). Together,
307 these results suggest that loss of small RNAs and telomerase elicits telomere damage
308 but not telomere fusions in early generations. The rapid sterility of these strains in later
309 generations occurs in response to end-to-end chromosome fusions that arise from
310 critically shortened telomeres.
311
312 We created a number of sRNA-deficient *trt-1* double mutants to define additional small
313 RNA factors that promote telomere stability in the absence of telomerase. The telomeric
314 sRNA pathway included RDE-4, which binds endogenous dsRNA and forms a complex
315 with the Dicer nuclease DCR-1, and the Argonaute RDE-1, which acts with the RNA-
316 dependent RNA polymerase RRF-3 to promote production of dsRNA-derived primary

317 sRNAs (Gent et al., 2010, Steiner et al., 2009, Tabara et al., 2002) (Figure 1B). The
318 MUTATOR proteins MUT-7 and MUT-14, which promote amplification of 22G
319 secondary sRNAs that can promote transcriptional silencing in the nucleus (Billi et al.,
320 2014, Ketting et al., 1999, Tijsterman et al., 2002), were also required to prevent rapid
321 sterility in *trt-1* mutants (Figure 1B). Two other small RNA factors, RRF-2 and ERI-1,
322 did not affect *trt-1* mutant sterility (Figure 1B), indicating that the endogenous 26G
323 sRNA pathway that requires ERI-1 (Gent et al., 2010, Han et al., 2009) is dispensable
324 for telomere stability in the absence of telomerase.
325
326 We crossed *dcr-1* and *mut-7* single mutants with wild-type males, singled F2 progeny
327 that were homozygous mutant for *dcr-1* or *mut-7*, and isolated genomic DNA from F4,
328 F6 and F8 generation descendants. Southern blotting revealed discrete telomere bands
329 that display modest telomere erosion for freshly homozygous *dcr-1* and *mut-7* mutant
330 telomeres (Figure S1A, B), although none of the small RNA single mutants we tested
331 became progressively sterile or accumulated chromosome fusions (Figure 1G). We
332 asked if the accelerated sterility of small RNA-deficient *trt-1* mutant strains might be
333 explained by short telomeres inherited from gametes derived from small RNA-deficient
334 grandparents using genetics, by crossing a *trt-1; dcr-1* double mutant hermaphrodite
335 with *dcr-1* mutant males, singling *trt-1 +/-; dcr-1 -/-* F1 hermaphrodites and isolating *trt-*
336 *1; dcr-1* double mutant F2. This cross was repeated 15 times to create a *trt-1; dcr-1*
337 double mutant strain whose telomeres should be exclusively derived from the *dcr-1*
338 mutant background. The *trt-1; dcr-1* 15x strain became sterile slightly slower than
339 freshly created *trt-1; dcr-1* double mutants, although this difference was not statistically
340 significant ($p = 0.07$) (Figure 1F). These results indicate that shortened telomeres
341 transmitted from the *dcr-1* mutant cannot explain the rapid sterility of *trt-1; dcr-1* double
342 mutants. We analyzed the dynamics of telomere erosion in sRNA-deficient *trt-1* mutant
343 strains using terminal restriction fragment analysis but did not observe a significant
344 difference in the rate of telomere erosion when passaging multiple worms per plate, in
345 comparison to *trt-1* single mutant controls ($p > 0.7$ in both cases) (Figure S1A, B).
346 However, when we passaged individual worms for each genotype, we observed
347 significant levels of telomere instability in sRNA-deficient *trt-1* mutant strains in

348 comparison to *trt-1* single mutant controls. Southern blotting revealed that *trt-1; mut-7*
349 and *trt-1; dcr-1* mutants had a significantly larger variance in the rate of telomere
350 erosion than *trt-1* mutants, which resulted from atypical shortening and elongation
351 events (Figure S2A, B).
352
353 We hypothesized that small RNAs might repress rapid sterility by directing chromatin
354 factors to telomeres to promote deposition of heterochromatic marks. *C. elegans*
355 telomeres have previously been reported to be enriched for H3K9me2 and bound by the
356 HP1 homolog HPL-2, which promotes H3K9me2 deposition and heterochromatin
357 formation, but not by the other *C. elegans* HP1 homolog HPL-1, which interacts with
358 H3K9me3 (Canzio et al., 2014, McMurchy et al., 2017). We confirmed that H3K9me2
359 but not H3K9me3 was enriched at *C. elegans* telomeres using high throughput
360 sequencing data sets generated from chromatin immunoprecipitation (ChIP)
361 experiments performed by independent groups (McMurchy et al., 2017, Zeller et al.,
362 2016). Moreover, we observed small H3K9me2 domains that extended into the
363 subtelomere at all *C. elegans* chromosome ends (Figure 3A-C). Similar to primary and
364 secondary sRNA-deficient *trt-1* strains, loss of HPL-2 but not HPL-1 caused accelerated
365 senescence in *trt-1* mutants (Figure 1C). H3K4 methylation, which is associated with
366 regions of active transcription, must be removed by demethylases prior to deposition of
367 repressive H3K9 methylation (Greer et al., 2010, Li et al., 2008). We found that loss of
368 either of the two *C. elegans* H3K4 demethylases RBR-2/KDM5 or SPR-5/LSD1 caused
369 rapid sterility of *trt-1* mutants (Figure 1C). Thus, H3K4 demethylation and H3K9me2
370 deposition prevent telomere instability in the absence of telomerase.
371
372 The histone remodeling protein XNP-1/ATRX has previously been implicated in
373 telomeric heterochromatin formation and interacts with unmethylated H3K4 and
374 methylated H3K9 deposited on the histone variant H3.3 (Udugama et al., 2015). *trt-1*
375 *xnp-1* double mutants became sterile significantly faster than *trt-1* single mutants but not
376 as fast as small RNA deficient *trt-1; mut-7* double mutants (Figure 1D). As loss of both
377 *xnp-1* and *mut-7* did not exacerbate the accelerated sterility phenotype of sRNA-
378 deficient *trt-1* mutant strains (Figure 1D), these genes function in the same telomere

379 stability pathway. This suggests that XNP-1 mediates some, but not all, of the small
380 RNA response to DNA damage at telomeres, possibly because sRNA-dependent
381 methylation of histones other than H3.3, such as canonical histone H3, can promote
382 telomere stability.
383
384 **Increased expression of TERRA in small RNA and chromatin deficient *trt-1* strains**
385 We hypothesized that DCR-1 and RDE-4 may interact with telomeric dsRNA produced
386 from bidirectional transcription of telomeres or interstitial telomere sequences to create
387 primary sRNAs that are then amplified into a secondary sRNA population that triggers
388 small RNA-dependent silencing of TERRA (Rossiello et al., 2017, Vrbsky et al., 2010).
389 To test whether small RNA and chromatin factors regulate telomeric transcription we
390 measured the abundance of TERRA by qRT-PCR at three chromosome ends using
391 primers within their H3K9me2-coated subtelomere domains (Figure 3A-C). Compared
392 to *trt-1* single mutant controls, TERRA was upregulated in early-generations in three
393 strains - *trt-1; rde-4* and *trt-1; mut-14* and *trt-1; spr-5* double mutants - but not in *trt-1* or
394 sRNA-deficient single mutant controls (Figure 2A). These results are distinct from
395 previous observations that show that TERRA transcription can be specifically induced at
396 damaged or shortened telomeres of mammalian cells that possess telomerase (Porro et
397 al., 2014, Rossiello et al., 2017).
398
399 We next used RNA Fluorescence *In Situ* Hybridization (FISH) to confirm the effects on
400 TERRA expression and to examine its cell and tissue localization. In wild-type control
401 and *trt-1* mutant hermaphrodite and male worms, TERRA was expressed at low levels
402 in the soma as well as in the pachytene region of the meiotic germline (Figures 2B-D,
403 S3-4), which corresponds to the location of several lncRNA-mediated germline silencing
404 processes (Taylor et al., 2015), including Meiotic Silencing of Sex Chromosomes in
405 mammals and *C. elegans* (Heard and Turner, 2011) and a transcriptional burst of
406 piRNAs in mammals that primes genomic silencing in germ cells prior to gametogenesis
407 (Gou et al., 2014). Compared to both wild-type control and *trt-1* or *dcr-1* single mutant
408 strains, *trt-1; dcr-1* double mutant strains had increased expression of TERRA in the
409 germline (Figures 2B-D, S3) and soma (Figures S3-4) by the F6 generation. We

410 observed an increase in the number of TERRA foci per nucleus in sRNA-deficient *trt-1*
411 mutants, which are likely to occur at telomeres (Figure 2D). We also observed TERRA
412 expression by RNA FISH in the cytoplasm and nucleoplasm of sRNA-deficient *trt-1* cells
413 (Figure 2B-C, S3), which might be consistent with possible non-telomeric functions of
414 TERRA (Chu et al., 2017, Roake and Artandi, 2017) or with a role for TERRA in
415 protecting telomeres *in trans* (Montero et al., 2018). This suggests that endogenous
416 sRNAs may repress telomeric transcription in the absence of telomerase, although it is
417 possible that subtelomeric transcription increases in sRNA-deficient telomerase mutants
418 in response to telomeric DNA damage (Figure 1H).
419
420 **Subtelomeric sRNAs are upregulated in telomerase mutants**
421 Telomeric sRNAs have been observed in protists, plants, and mammals (Cao et al.,
422 2009, Couvillion et al., 2009, Vrbsky et al., 2010). We recently interrogated 92 publicly
423 available small RNA sequencing libraries created from RNA isolated from various *C.*
424 *elegans* strains and found rare reads that mapped perfectly to the *C. elegans* telomere
425 repeat $(TTAGGC)_n$, occurring at a frequency of 1 per 10,000,000 reads (Frenk et al.,
426 2019). piRNAs with up to 3 mismatches can target regions of the *C. elegans* genome for
427 silencing (Bagijn et al., 2012), and we found that telomeric sRNAs with up to 3
428 mismatches were substantially more abundant than those with perfect telomere repeat
429 sequence (1 per 100,000) (Frenk et al., 2019). We compared levels of telomeric sRNAs
430 with mismatches from wildtype with those of mutants for small RNA genes that promote
431 telomere stability in the absence of telomerase, such as *dcr-1*, *rde-4*, *mut-7*, and *mut-*
432 *14*, and found that levels of telomeric sRNAs were sometimes depleted in these
433 backgrounds, but not always (File S1).
434
435 We asked if loss of telomerase might alter levels of telomeric sRNAs in a manner that
436 might depend on Dicer by isolating RNA from wild-type control, *trt-1* single mutant, and
437 *trt-1; dcr-1* double mutant strains and preparing small RNA libraries. We sequenced
438 these libraries deeply in an effort to detect rare perfect telomeric sRNAs. We obtained
439 ~20,000,000 reads each for 6 data sets and found that our *trt-1; dcr-1* data sets were
440 strongly depleted of 22G RNAs that were previously reported to depend on *dcr-1*

441 (Figure S5A) (Gent et al., 2010). To assess TRT-1-dependent changes in sRNAs
442 throughout the genome, we counted the number of 22G reads mapping uniquely
443 antisense to protein-coding genes and found upregulation of sRNAs at 720 loci and
444 downregulation at 456 loci in *trt-1* animals compared with wild-type controls (Figure
445 S5B). Of the upregulated loci, 465 were not upregulated in *trt-1; dcr-1* animals
446 compared with wildtype, indicating DCR-1 dependence. We did not find significant GO
447 terms in loci with either up or downregulated sRNA production. Given that *trt-1* is
448 expressed at high levels in *C. elegans* germ cells (Meier et al., 2006), we asked whether
449 the loci with differential sRNA production were enriched for germline-enriched genes.
450 We used previously published data on germline expression (Ortiz et al., 2014) and
451 found significant enrichment for germline-enriched genes in both upregulated and
452 downregulated loci ($p < 1e-19$ and $p < 1e-33$ respectively, Pearson's Chi Square test
453 with Bonferroni correction) (Figure S5C). This may reflect an epigenetic response to
454 deficiency for telomerase in germ cells, even though early-generation *trt-1* mutants from
455 which the RNA was prepared had normal levels of fertility. sRNAs mapping to
456 transposons were unaffected by loss of TRT-1, with the exception of the CER-10 LTR
457 retrotransposon, for which sRNAs were three-fold downregulated (Figure S5D).
458
459 We found that levels of telomeric sRNAs with 1 to 3 mismatches did not change
460 substantially in sRNAs from *trt-1* single mutants or *trt-1; dcr-1* double mutants, but
461 detected no sRNAs composed of perfect telomere repeats in any genetic background
462 (Figure 4A). We next examined 22G RNAs at subtelomeric regions (defined as 2kb of
463 sequence adjacent to each telomere) and found that these were present in wild-type
464 samples at the left end of chromosome *III*, and that their abundance was increased two-
465 fold in *trt-1* single mutants and their presence almost entirely eliminated in *trt-1; dcr-1*
466 double mutants (Figure 4C, E). Subtelomeric sRNAs were also observed within 1kb of
467 the telomere at the left ends of chromosomes *I* and *IV* in *trt-1* mutants and not in
468 wildtype or *trt-1; dcr-1* double mutants (Figure 4B, D). The right ends of Chromosomes *I*
469 and *III* and the left end of Chromosome *II* all showed at least a two-fold increase in
470 subtelomeric sRNAs in *trt-1* and/or *trt-1; dcr-1* double mutants (Figure 4E). We
471 observed a significant bias for subtelomeric sRNAs whose sequences correspond to the

472 C-rich telomere strand (antisense to TERRA) for the left ends of Chromosomes *I* and *III*
473 ($p < 1e-13$ and $p < 1e-43$ respectively, binomial test with Bonferroni correction) and for
474 the right arm of Chromosome *I* ($p < 1e-172$, binomial test with Bonferroni correction)
475 while the nucleotide sequences of subtelomeric sRNAs at the left arm of Chromosome
476 *IV* and the right arm of Chromosome *III* showed a bias for subtelomeric TERRA,
477 suggesting that they were created from RNA containing the C-rich telomeric sequence
478 ($p < 1e-11$, $p = 0.006$ respectively, binomial test with Bonferroni correction) (Figure 4F).
479 These observations suggest that telomere dysfunction triggers the upregulation of small
480 RNA biogenesis at multiple subtelomeres through both DCR-1-dependent and -
481 independent mechanisms. sRNA biogenesis might be induced at a subset of
482 subtelomeres when telomerase is dysfunctional because 1) shortened telomeres
483 inherited from *trt-1* mutant gametes that created *trt-1* single mutants might trigger sRNA
484 biogenesis, or 2) DNA damage that occurs stochastically at specific subtelomeres elicits
485 sRNA biogenesis. Subtelomeric siRNAs that correspond to the G- or C-rich telomeric
486 strand at specific subtelomeres could be related to the presence of transcripts that can
487 be targeted for sRNA biogenesis at these telomeres.
488
489 We next interrogated data sets of small RNAs that immunoprecipitate with Argonaute
490 proteins that are known to promote silencing in the germline, HRDE-1 and WAGO-1, as
491 well as with the germline anti-silencing Argonaute CSR-1 (Gu et al., 2009, Claycomb et
492 al., 2009, Ashe et al., 2012). Enrichment of small RNAs for each protein was calculated
493 by dividing the number of reads in the immunoprecipitate library by the number of reads
494 in the corresponding input library. Telomeric sRNAs were enriched in WAGO-1
495 immunoprecipate relative to input, but this was not the case for HRDE-1 or CSR-1
496 (Figure 3D). Enrichment of subtelomeric small RNAs in WAGO-1 was detected at all
497 chromosome ends tested apart from the right arm of Chromosome *I* (some
498 chromosome ends were not tested due to an absence of reads in the input library).
499 Enrichment was also detected for HRDE-1 at all chromosome ends excluding the right
500 arm of Chromosome *I* and the left arm of Chromosome *III* (Figure 3E). Interestingly,
501 CSR-1 showed the opposite pattern of enrichment to WAGO-1 and HRDE-1, with
502 enrichment at none of the chromosome ends apart from the right end of Chromosome *I*.

503 The ribosomal DNA, the most highly expressed locus in the *C. elegans* genome, is
504 immediately adjacent to this telomere (Wicky et al., 1996), and it is therefore possible
505 that sRNA activity takes a predominantly anti-silencing function at this chromosome
506 end. We asked if either Argonaute that associates with telomeric or sub-telomeric
507 sRNAs, WAGO-1 or to a lesser degree HRDE-1, promotes telomere maintenance in the
508 absence of telomerase and found that *wago-1 trt-1* and *trt-1; hrde-1* double mutants
509 both displayed rapid sterility phenotypes in comparison to *trt-1* single mutants ($p < 1e-$
510 11 and $p < 1e-12$, respectively, log rank test) (Figure 1E).
511
512 **Telomeric sRNAs and loss of EXO-1 repress sterility in the absence of telomerase**
513 We considered simultaneously targetting the 11 unique subtelomeres of the *C. elegans*
514 genome with exogenous subtelomeric sRNAs in an effort to show that this class of
515 sRNAs promotes telomere stability in the absence of telomerase, but felt that this might
516 be difficult. Therefore, we decided to test the hypothesis that telomere repeat sRNAs
517 can promote telomere stability in the absence of telomerase. We asked if introduction
518 of exogenous telomeric sRNAs could rescue the rapid sterility of sRNA-deficient *trt-1*
519 mutants using a viable *dcr-1* allele, *mg375*, which is deficient for endogenous sRNA
520 production but is hypersensitive to exogenous RNAi when fed *E. coli* expressing dsRNA
521 (Welker et al., 2010). *trt-1; dcr-1(mg375)* double mutant strains that were passaged on
522 bacteria expressing telomeric dsRNA remained fertile significantly longer than those
523 expressing dsRNA from an empty vector control (Figure 4A). In contrast, exogenous
524 telomeric dsRNA did not affect the onset of sterility for *trt-1* single mutant controls.
525 Moreover, *trt-1; dcr-1(mg375)* strains fed telomeric dsRNA had markedly reduced levels
526 of DNA damage at F6 in comparison to *trt-1; dcr-1(mg375)* strains grown on control
527 RNAi or on regular OP50 bacteria that do not express dsRNA (Figure 1F, 5C).
528
529 In budding yeast, artificially-induced TERRA overexpression promotes telomere
530 shortening *in cis* by forming RNA:DNA hybrids that stall telomeric replication forks in a
531 manner that stimulates telomere resection by the exonuclease Exo1 (Maicher et al.,
532 2012, Pfeiffer and Lingner, 2012). We therefore hypothesized that loss of EXO-1 might
533 rescue the accelerated sterility phenotype in sRNA-deficient telomerase mutants. *trt-1;*

534 *exo-1; mut-14* triple mutant lines survived significantly longer than *trt-1; mut-14* double
535 mutants (Figure 5B) and displayed reduced levels of DNA damage and moderate levels
536 of TERRA at generation F6 (Figures 5B, S5). Moreover, *trt-1; exo-1* double mutant
537 controls remained fertile even longer than *trt-1* single mutants (Figure 5B), indicating
538 that EXO-1-mediated telomere resection promotes telomere-shortening-induced
539 senescence in the absence of telomerase, both at normal telomeres and at telomeres
540 lacking sRNA-mediated genomic silencing. While *trt-1; exo-1* double mutant controls
541 remained fertile longer than *trt-1* single mutants, this was not true for *trt-1* single
542 mutants grown on exogenous telomeric dsRNA (Figure 5A, B). Thus, *exo-1* has at least
543 two roles at telomeres, one role that promotes sterility when telomerase is absent and a
544 second that promotes sterility when telomerase and sRNA silencing is absent.
545
546
547 **Discussion**
548 Small RNAs promote genomic silencing of many types of transposons (Holoch and
549 Moazed, 2015), including those found at *Drosophila melanogaster* telomeres, which are
550 composed of non-LTR retrotransposons that are distinct from the simple repetitive
551 sequences that are maintained by telomerase and cap chromosome ends in most
552 organisms (Pardue and DeBaryshe, 2003). Components of the RNAi machinery
553 function at *Drosophila* telomeres to repress expression of HeT-A and TART
554 retrotransposons and their accumulation at chromosome termini (Pane et al., 2007,
555 Savitsky et al., 2006), even though they do not affect telomere capping (Perrini et al.,
556 2004). In contrast, loss of the *Drosophila* homologs of the heterochromatin-mediated
557 genome silencing proteins HP1 and ATRX causes immediate telomere deprotection and
558 fusion (Chavez et al., 2017, Fanti et al., 1998, Fulcher et al., 2014). H3K9me2 but not
559 H3K9me3 is present at wild-type *C. elegans* telomeres (Figure 3A-C) (McMurchy et al.,
560 2017, Zeller et al., 2016), and we found that the *C. elegans* HP1 homolog HPL-2 that
561 binds to and specifically stabilizes H3K9me2 (McMurchy et al., 2017) promotes
562 telomere stability in the absence of telomerase (Figure1C). We also identified factors
563 that create rare small RNAs that may guide the deposition of histone silencing marks in
564 response to damaged telomeres (Figure 6A). Therefore, small RNAs and

565 heterochromatin proteins represent conserved features of both non-canonical and
566 canonical telomeres, even though their functions are distinct.
567
568 Loss of telomerase and sRNA factors in *C. elegans* caused high levels of DNA damage
569 response signaling in germ cells, but did not result in telomere fusions for a number of
570 generations, each generation representing 8-10 cell divisions. Therefore, the
571 accelerated sterility phenotype of sRNA-deficient *trt-1* mutants is not a consequence of
572 a defect in acute telomere uncapping, but rather an acceleration of the onset of crisis.
573 Biochemical analysis of telomere erosion in sRNA-deficient *trt-1* mutants revealed
574 increased variance in telomere size, which could be due to an error-prone
575 recombinational response to a form of DNA damage such as a stalled replication fork
576 (Figure 6C-D). Although both elongation and shortening of telomeres were observed
577 (Figure S1,S2), we propose that rapid telomere shortening events are likely responsible
578 for the premature end-to-end chromosome fusion and sterility phenotypes of sRNA-
579 deficient *trt-1* mutants. In telomerase single mutants that are proficient for sRNA
580 biogenesis and heterochromatin deposition, telomeric DNA damage may be healed in a
581 manner that more accurately maintains telomere length and is coupled to expression
582 and subsequent sRNA-mediated silencing of TERRA (Figure 6A-B).
583
584 Heterochromatin is known to suppress replication-based DNA damage at repetitive
585 segments of the genome (Zeller et al., 2016, Janssen et al., 2018). However, repeated
586 crossing of a *trt-1* mutation into a *dcr-1* mutant background failed to exacerbate the
587 accelerated sterility of *trt-1; dcr-1* double mutants (Figure 1F), indicating that *dcr-*
588 *1(mg375)* mutants have telomeres of normal length. Therefore, telomerase-mediated
589 telomere repeat addition is likely to be an effective method of healing telomeric DNA
590 damage in the absence of sRNA-mediated heterochromatin deposition.
591
592 Loss of telomeric sRNA biogenesis in telomerase mutants resulted in TERRA
593 expression, which could create R-loops that induce homologous recombination in a
594 manner that creates telomere shortening events that are toxic (Figure 6C). As
595 exogenous telomeric sRNAs were sufficient to suppress telomere instability, DNA

596 damage signaling and TERRA expression in the absence of telomerase and
597 endogenous sRNAs (Figure 5), silencing of TERRA could be an integral part of a
598 telomeric DNA damage response (Figure 6B,D) (Toubiana and Selig, 2018). These
599 results are consistent with a role for TERRA expression in response to a distinct form of
600 telomeric damage that occurs in the presence of telomerase – acutely deprotected, non-
601 replicating telomeres – and is accompanied by production of telomeric sRNAs that
602 promote DNA damage response factor recruitment (Rossiello et al., 2017). In addition,
603 work in *S. cerevisiae* showed that increased TERRA expression and persistent
604 telomeric R-loops in telomerase mutants can repress senescence by promoting
605 recombination, indicating that increased levels of TERRA are coupled to induction of a
606 telomeric DNA damage response (Graf et al., 2017). Finally, elevated levels of TERRA
607 have been shown to contribute to senescence in *S. cerevisiae* (Wanat et al., 2018).
608
609 We observed reduced levels of TERRA and DNA damage signaling in sRNA-deficient
610 telomerase mutants that lack *exo-1*. Consistently, loss of EXO1 in telomerase-negative
611 mice has been shown to extend lifespan and improve organ maintenance by repressing
612 telomeric ssDNA formation and DNA damage response (Schaetzlein et al., 2007),
613 suggesting a conserved role for EXO1 in the metazoan response to dysfunctional
614 telomeres. Although expression of TERRA at mammalian telomeres induces EXO1-
615 dependent telomere shortening in a manner that independent of RNase H (Pfeiffer and
616 Lingner, 2012), we did not test a role for RNase H in the telomere instability phenotype
617 of sRNA-deficient *C. elegans* telomerase mutants.
618
619 We previously observed that *C. elegans* telomeric sRNAs with mismatches can be
620 mapped to Interstitial Telomere Sequences, which are degenerate telomere tracts that
621 are abundant on chromosomes arms and are distinct from telomeres (Frenk et al.,
622 2019). Interstitial Telomere Sequences were often heterochromatic and were markedly
623 depleted from exons and 5' or 3' UTRs (Frenk et al., 2019). Telomeric sRNAs with
624 mismatches were not altered by the *dcr-1(mg375)* mutation that causes telomere
625 instability in the absence of telomerase (Figure 4A). Although telomeric sRNAs with
626 mismatches contained a mixture of all four 5' nucleotides, very rare sRNAs composed

627 of perfect telomere repeats were strongly depleted for 5' G nucleotides (Frenk et al.,
628 2019). The unique structural property suggests a mechanism of biogenesis that is
629 distinct from known classes of *C. elegans* sRNAs (Billi et al., 2014). We found that
630 perfect telomeric sRNAs from the environment were sufficient to promote telomere
631 stability in *trt-1; dcr-1* mutants (Figure 5A). This suggests that very rare perfect
632 telomeric small RNAs, which might appear fleeting or artefactual based on analysis of
633 RNA sequencing data sets, promote telomere stability in the absence of telomerase.
634 Similar classes of rare small RNAs, which may be difficult (Frenk et al., 2019) or
635 impossible (Figure 4A) to measure, could be relevant to other segments of the genome.
636
637 As both Dicer and the dsRNA-binding protein RDE-4 promoted telomere stability in the
638 absence of telomerase (Figure 1B), we propose that biogenesis of telomeric small
639 RNAs could involve bidirectional transcripts that emanate from ITS tracts at internal
640 segments of the genome to create dsRNAs that contain both perfect and imperfect
641 telomere repeats (Frenk et al., 2019). ITS dsRNAs could interact with RDE-4 and Dicer
642 to create primary and secondary sRNA populations that could interact with TERRA
643 (Figure 6A). We detected subtelomeric sRNAs that were dependent on Dicer and that
644 interacted with the Argonaute proteins WAGO-1 and HRDE-1, both of which promoted
645 telomere stability in the absence of telomerase. These Argonaute proteins are known to
646 act in germ cells to target overlapping groups of transcripts, including genes,
647 transposons, and pseudogenes (Gu et al., 2009). Although WAGO-1 localizes to
648 perinuclear P-granules (germ granules), where it might promote either transcriptional or
649 post-transcriptional gene silencing (Gu et al., 2009), HRDE-1 localizes to the nucleus
650 where it promotes transcriptional gene silencing. Moreover, HRDE-1 and WAGO-1
651 have been shown to function redundantly to promote a form of permanent
652 transgenerational transcriptional silencing (Ashe et al., 2012, Buckley et al., 2012).
653 Although proteomics has been performed for both HRDE-1 and WAGO-1, they do not
654 physically interact with one another or possess common interacting proteins (Akay et
655 al., 2017, Shirayama et al., 2014).
656

657 We were unable to measure perfect telomeric sRNAs by deeply sequencing small
658 RNAs from several genetic backgrounds (Figure 4A), but we observed upregulation of
659 sRNAs at some subtelomeres in telomerase mutants, and in some cases this increase
660 was DCR-1-dependent (Figure 4). We also found that HRDE-1 and WAGO-1 interact
661 with 22G sRNAs that map to distinct and overlapping subtelomeres. Given that DNA
662 damage responses induce histone modifications that can be propagated for long
663 distances from sites of DNA damage (Polo and Jackson, 2011), we propose that the
664 biological response to telomeric DNA damage initially may spread such that abundant
665 sRNAs are created from RNA transcripts at some subtelomeric loci. Therefore, the
666 variable sRNA biogenesis patterns observed at distinct subtelomeres of telomerase
667 mutants may reflect a wider epigenetic consequence of the biological response to
668 telomeric DNA damage.
669
670 In mammals, TERRA facilitates transcriptional regulation of the epigenome (Chu et al.,
671 2017). Moreover, both TERRA and telomerase have been implicated in regulation of
672 genes that promote stem cell proliferation (Marion et al., 2019, Sarin et al., 2005).
673 Therefore, the interplay of telomerase and TERRA in the context of deficiency for small
674 RNA-mediated genome silencing could reflect more general roles for these factors in
675 epigenetic regulation of cell fate.
676
677 sRNA-mediated telomeric silencing was promoted by the *C. elegans* secondary sRNA
678 biogenesis factor MUT-7 (Figure 1A, B), which is homologous to the exonuclease
679 domain of human WRN1 Werner's syndrome protein whose loss results in early-onset
680 aging of multiple tissues (Ketting et al., 2001). WRN1 deficiency is accompanied by
681 accelerated telomere erosion and senescence phenotypes that can be rescued by
682 telomerase expression (Shimamoto et al., 2015). While WRN1 and its homologs have
683 been intensively studied for their roles in DNA recombination, WRN1 safeguards the
684 stability of heterochromatin (Zhang et al., 2015), which our study suggests may play a
685 critical role in maintaining telomere stability in most human somatic cells. Consistently,
686 deficiency for DNA methylation at repetitive segments of the genome, including
687 telomeres, occurs in ICF syndrome cells that undergo rapid telomere shortening and

688 senescence accompanied by increased TERRA expression, telomeric R-loops and DNA
689 damage (Sagie et al., 2017). As global dysfunction of the epigenome is a hallmark of
690 human aging (Zhang et al., 2015), our findings may be generally relevant to
691 understanding how sRNA-driven chromatin states established in germ cells or the early
692 embryo might contribute to telomere instability during aging of adult somatic cells.
693

694 **Data availability statement**

695 RNA-seq data reported in this study are available under the accession number GEO:
696 GSE111800.
697

698 **Acknowledgements**

699 We thank R. Dowen for technical advice with qRT-PCR, K. Billmyre for advice on
700 immunofluorescence, and members of the S.A. laboratory for critical review of the
701 manuscript. Some strains were provided by the *Caenorhabditis* Genetics Center, which
702 is funded by National Institutes of Health Office of Research Infrastructure Programs
703 (P40 OD010440).
704

705 **Funding**

706 S.F., C.L. and S.A. were supported by National Institute of Health grant R01 GM135470
707 and R01 ES035777.
708

709 **Conflict of Interest**

710 The authors declare no competing interests.

711 **References**
712

713 AHMED, S. & HODGKIN, J. 2000. MRT-2 checkpoint protein is required for germline
714 immortality and telomere replication in *C. elegans*. *Nature,* 403**,** 159-64.
715 AKAY, A., DI DOMENICO, T., SUEN, K. M., NABIH, A., PARADA, G. E., LARANCE,
716 M., MEDHI, R., BERKYUREK, A. C., ZHANG, X., WEDELES, C. J., RUDOLPH,
717 K. L. M., ENGELHARDT, J., HEMBERG, M., MA, P., LAMOND, A. I.,
718 CLAYCOMB, J. M. & MISKA, E. A. 2017. The Helicase Aquarius/EMB-4 Is
719 Required to Overcome Intronic Barriers to Allow Nuclear RNAi Pathways to
720 Heritably Silence Transcription. *Dev Cell,* 42**,** 241-255 e6.
721 ARNOULT, N., VAN BENEDEN, A. & DECOTTIGNIES, A. 2012. Telomere length
722 regulates TERRA levels through increased trimethylation of telomeric H3K9 and
723 HP1alpha. *Nat Struct Mol Biol,* 19**,** 948-56.
724 ASHE, A., SAPETSCHNIG, A., WEICK, E. M., MITCHELL, J., BAGIJN, M. P.,
725 CORDING, A. C., DOEBLEY, A. L., GOLDSTEIN, L. D., LEHRBACH, N. J., LE
726 PEN, J., PINTACUDA, G., SAKAGUCHI, A., SARKIES, P., AHMED, S. & MISKA,
727 E. A. 2012. piRNAs Can Trigger a Multigenerational Epigenetic Memory in the
728 Germline of C. elegans. *Cell,* 150**,** 88-99.
729 AVGOUSTI, D. C., PALANI, S., SHERMAN, Y. & GRISHOK, A. 2012. CSR-1 RNAi
730 pathway positively regulates histone expression in C. elegans. *EMBO J,* 31**,**
731 3821-32.
732 AZZALIN, C. M. & LINGNER, J. 2015. Telomere functions grounding on TERRA firma.
733 *Trends Cell Biol,* 25**,** 29-36.
734 AZZALIN, C. M., REICHENBACH, P., KHORIAULI, L., GIULOTTO, E. & LINGNER, J.
735 2007. Telomeric repeat containing RNA and RNA surveillance factors at
736 mammalian chromosome ends. *Science,* 318**,** 798-801.
737 BAGIJN, M. P., GOLDSTEIN, L. D., SAPETSCHNIG, A., WEICK, E. M., BOUASKER,
738 S., LEHRBACH, N. J., SIMARD, M. J. & MISKA, E. A. 2012. Function, targets,
739 and evolution of Caenorhabditis elegans piRNAs. *Science,* 337**,** 574-8.
740 BATISTA, P. J., RUBY, J. G., CLAYCOMB, J. M., CHIANG, R., FAHLGREN, N.,
741 KASSCHAU, K. D., CHAVES, D. A., GU, W., VASALE, J. J., DUAN, S., CONTE,
742 D., JR., LUO, S., SCHROTH, G. P., CARRINGTON, J. C., BARTEL, D. P. &
743 MELLO, C. C. 2008. PRG-1 and 21U-RNAs interact to form the piRNA complex
744 required for fertility in C. elegans. *Mol Cell,* 31**,** 67-78.
745 BENETTI, R., GARCIA-CAO, M. & BLASCO, M. A. 2007. Telomere length regulates the
746 epigenetic status of mammalian telomeres and subtelomeres. *Nat Genet,* 39**,**
747 243-50.
748 BENETTI, R., SCHOEFTNER, S., MUNOZ, P. & BLASCO, M. A. 2008. Role of TRF2 in
749 the assembly of telomeric chromatin. *Cell Cycle,* 7**,** 3461-8.
750 BERNSTEIN, E., CAUDY, A. A., HAMMOND, S. M. & HANNON, G. J. 2001. Role for a
751 bidentate ribonuclease in the initiation step of RNA interference. *Nature,* 409**,**
752 363-6.
753 BILLI, A. C., FISCHER, S. E. & KIM, J. K. 2014. Endogenous RNAi pathways in C.
754 elegans. *WormBook***,** 1-49.
755 BOERCKEL, J., WALKER, D. & AHMED, S. 2007. The Caenorhabditis elegans Rad17
756 homolog HPR-17 is required for telomere replication. *Genetics,* 176**,** 703-9.

BUCKLEY, B. A., BURKHART, K. B., GU, S. G., SPRACKLIN, G., KERSHNER, A., FRITZ, H., KIMBLE, J., FIRE, A. & KENNEDY, S. 2012. A nuclear Argonaute promotes multigenerational epigenetic inheritance and germline immortality. *Nature,* 489**,** 447-51.

BUSHNELL, B. 2016. BBMap short-read aligner, and other bioinformatics tools. http://sourceforge.net/projects/bbmap/.

CANZIO, D., LARSON, A. & NARLIKAR, G. J. 2014. Mechanisms of functional promiscuity by HP1 proteins. *Trends Cell Biol,* 24**,** 377-86.

CAO, F., LI, X., HIEW, S., BRADY, H., LIU, Y. & DOU, Y. 2009. Dicer independent small RNAs associate with telomeric heterochromatin. *RNA,* 15**,** 1274-81.

CHAVEZ, J., MURILLO-MALDONADO, J. M., BAHENA, V., CRUZ, A. K., CASTANEDA-SORTIBRAN, A., RODRIGUEZ-ARNAIZ, R., ZURITA, M. & VALADEZ-GRAHAM, V. 2017. dAdd1 and dXNP prevent genome instability by maintaining HP1a localization at Drosophila telomeres. *Chromosoma,* 126**,** 697-712.

CHENG, C., SHTESSEL, L., BRADY, M. M. & AHMED, S. 2012. Caenorhabditis elegans POT-2 telomere protein represses a mode of alternative lengthening of telomeres with normal telomere lengths. *Proc Natl Acad Sci U S A,* 109**,** 7805-10.

CHU, H. P., CIFUENTES-ROJAS, C., KESNER, B., AEBY, E., LEE, H. G., WEI, C., OH, H. J., BOUKHALI, M., HAAS, W. & LEE, J. T. 2017. TERRA RNA Antagonizes ATRX and Protects Telomeres. *Cell,* 170**,** 86-101 e16.

CLAYCOMB, J.M., BATISTA, P.J., PANG, K.M., GU, W., VASALE, J.J., VAN WOLFSWINKEL, J.C., CHAVES, D.A., SHIRAYAMA, M., MITANI, S., KETTING, R.F., CONTE D., MELLO C.C. (2009). The Argonaute CSR-1 and its 22G-RNA cofactors are required for holocentric chromosome segregation. *Cell* 139, 123-134.

COUVILLION, M. T., LEE, S. R., HOGSTAD, B., MALONE, C. D., TONKIN, L. A., SACHIDANANDAM, R., HANNON, G. J. & COLLINS, K. 2009. Sequence, biogenesis, and function of diverse small RNA classes bound to the Piwi family proteins of Tetrahymena thermophila. *Genes Dev,* 23**,** 2016-32.

CUSANELLI, E., ROMERO, C. A. & CHARTRAND, P. 2013. Telomeric noncoding RNA TERRA is induced by telomere shortening to nucleate telomerase molecules at short telomeres. *Mol Cell,* 51**,** 780-91.

DAS, P. P., BAGIJN, M. P., GOLDSTEIN, L. D., WOOLFORD, J. R., LEHRBACH, N. J., SAPETSCHNIG, A., BUHECHA, H. R., GILCHRIST, M. J., HOWE, K. L., STARK, R., MATTHEWS, N., BEREZIKOV, E., KETTING, R. F., TAVARE, S. & MISKA, E. A. 2008. Piwi and piRNAs act upstream of an endogenous siRNA pathway to suppress Tc3 transposon mobility in the Caenorhabditis elegans germline. *Mol Cell,* 31**,** 79-90.

DONATE, L. E. & BLASCO, M. A. 2011. Telomeres in cancer and ageing. *Philos Trans R Soc Lond B Biol Sci,* 366**,** 76-84.

FANTI, L., GIOVINAZZO, G., BERLOCO, M. & PIMPINELLI, S. 1998. The heterochromatin protein 1 prevents telomere fusions in Drosophila. *Mol Cell,* 2**,** 527-38.

FLYNN, R. L., COX, K. E., JEITANY, M., WAKIMOTO, H., BRYLL, A. R., GANEM, N. J., BERSANI, F., PINEDA, J. R., SUVA, M. L., BENES, C. H., HABER, D. A.,

802 BOUSSIN, F. D. & ZOU, L. 2015. Alternative lengthening of telomeres renders
803 cancer cells hypersensitive to ATR inhibitors. *Science,* 347**,** 273-7.
804 FRENK, S., LISTER-SHIMAUCHI, E. H. & AHMED, S. 2019. Telomeric small RNAs in
805 the genus Caenorhabditis. *RNA*.
806 FULCHER, N., DERBOVEN, E., VALUCHOVA, S. & RIHA, K. 2014. If the cap fits, wear
807 it: an overview of telomeric structures over evolution. *Cell Mol Life Sci,* 71**,** 847-
808 65.
809 GENT, J. I., LAMM, A. T., PAVELEC, D. M., MANIAR, J. M., PARAMESWARAN, P.,
810 TAO, L., KENNEDY, S. & FIRE, A. Z. 2010. Distinct phases of siRNA synthesis
811 in an endogenous RNAi pathway in C. elegans soma. *Mol Cell,* 37**,** 679-89.
812 GOU, L. T., DAI, P., YANG, J. H., XUE, Y., HU, Y. P., ZHOU, Y., KANG, J. Y., WANG,
813 X., LI, H., HUA, M. M., ZHAO, S., HU, S. D., WU, L. G., SHI, H. J., LI, Y., FU, X.
814 D., QU, L. H., WANG, E. D. & LIU, M. F. 2014. Pachytene piRNAs instruct
815 massive mRNA elimination during late spermiogenesis. *Cell Res,* 24**,** 680-700.
816 GRAF, M., BONETTI, D., LOCKHART, A., SERHAL, K., KELLNER, V., MAICHER, A.,
817 JOLIVET, P., TEIXEIRA, M. T. & LUKE, B. 2017. Telomere Length Determines
818 TERRA and R-Loop Regulation through the Cell Cycle. *Cell,* 170**,** 72-85 e14.
819 GREER, E. L., MAURES, T. J., HAUSWIRTH, A. G., GREEN, E. M., LEEMAN, D. S.,
820 MARO, G. S., HAN, S., BANKO, M. R., GOZANI, O. & BRUNET, A. 2010.
821 Members of the H3K4 trimethylation complex regulate lifespan in a germline-
822 dependent manner in C. elegans. *Nature,* 466**,** 383-7.
823 GU, W., SHIRAYAMA, M., CONTE, D., JR., VASALE, J., BATISTA, P. J., CLAYCOMB,
824 J. M., MORESCO, J. J., YOUNGMAN, E. M., KEYS, J., STOLTZ, M. J., CHEN,
825 C. C., CHAVES, D. A., DUAN, S., KASSCHAU, K. D., FAHLGREN, N., YATES,
826 J. R., 3RD, MITANI, S., CARRINGTON, J. C. & MELLO, C. C. 2009. Distinct
827 argonaute-mediated 22G-RNA pathways direct genome surveillance in the C.
828 elegans germline. *Mol Cell,* 36**,** 231-44.
829 HAHNE, F. & IVANEK, R. 2016. Visualizing Genomic Data Using Gviz and
830 Bioconductor. *Methods Mol Biol,* 1418**,** 335-51.
831 HAN, T., MANOHARAN, A. P., HARKINS, T. T., BOUFFARD, P., FITZPATRICK, C.,
832 CHU, D. S., THIERRY-MIEG, D., THIERRY-MIEG, J. & KIM, J. K. 2009. 26G
833 endo-siRNAs regulate spermatogenic and zygotic gene expression in
834 Caenorhabditis elegans. *Proc Natl Acad Sci U S A,* 106**,** 18674-9.
835 HEARD, E. & TURNER, J. 2011. Function of the sex chromosomes in mammalian
836 fertility. *Cold Spring Harb Perspect Biol,* 3**,** a002675.
837 HOLOCH, D. & MOAZED, D. 2015. RNA-mediated epigenetic regulation of gene
838 expression. *Nat Rev Genet,* 16**,** 71-84.
839 HOLOHAN, B., WRIGHT, W. E. & SHAY, J. W. 2014. Cell biology of disease:
840 Telomeropathies: an emerging spectrum disorder. *J Cell Biol,* 205**,** 289-99.
841 JANSSEN, A., COLMENARES, S. U. & KARPEN, G. H. 2018. Heterochromatin:
842 Guardian of the Genome. *Annu Rev Cell Dev Biol,* 34**,** 265-288.
843 KASPER, D. M., GARDNER, K. E. & REINKE, V. 2014. Homeland security in the C.
844 elegans germ line: insights into the biogenesis and function of piRNAs.
845 *Epigenetics,* 9**,** 62-74.
846 KETTING, R. F., FISCHER, S. E., BERNSTEIN, E., SIJEN, T., HANNON, G. J. &
847 PLASTERK, R. H. 2001. Dicer functions in RNA interference and in synthesis of

848 small RNA involved in developmental timing in C. elegans. *Genes Dev,* 15**,** 2654-
849 9.
850 KETTING, R. F., HAVERKAMP, T. H., VAN LUENEN, H. G. & PLASTERK, R. H. 1999.
851 Mut-7 of C. elegans, required for transposon silencing and RNA interference, is a
852 homolog of Werner syndrome helicase and RNaseD. *Cell,* 99**,** 133-41.
853 KNIGHT, S. W. & BASS, B. L. 2001. A role for the RNase III enzyme DCR-1 in RNA
854 interference and germ line development in Caenorhabditis elegans. *Science,*
855 293**,** 2269-71.
856 LANGMEAD, B., TRAPNELL, C., POP, M. & SALZBERG, S. L. 2009. Ultrafast and
857 memory-efficient alignment of short DNA sequences to the human genome.
858 *Genome Biol,* 10**,** R25.
859 LI, F., HUARTE, M., ZARATIEGUI, M., VAUGHN, M. W., SHI, Y., MARTIENSSEN, R. &
860 CANDE, W. Z. 2008. Lid2 is required for coordinating H3K4 and H3K9
861 methylation of heterochromatin and euchromatin. *Cell,* 135**,** 272-83.
862 LI, J. S., MIRALLES FUSTE, J., SIMAVORIAN, T., BARTOCCI, C., TSAI, J.,
863 KARLSEDER, J. & LAZZERINI DENCHI, E. 2017. TZAP: A telomere-associated
864 protein involved in telomere length control. *Science,* 355**,** 638-641.
865 LOVE, M. I., HUBER, W. & ANDERS, S. 2014. Moderated estimation of fold change
866 and dispersion for RNA-seq data with DESeq2. *Genome Biol,* 15**,** 550.
867 LOVEJOY, C. A., LI, W., REISENWEBER, S., THONGTHIP, S., BRUNO, J., DE
868 LANGE, T., DE, S., PETRINI, J. H., SUNG, P. A., JASIN, M., ROSENBLUH, J.,
869 ZWANG, Y., WEIR, B. A., HATTON, C., IVANOVA, E., MACCONAILL, L.,
870 HANNA, M., HAHN, W. C., LUE, N. F., REDDEL, R. R., JIAO, Y., KINZLER, K.,
871 VOGELSTEIN, B., PAPADOPOULOS, N., MEEKER, A. K. & CONSORTIUM, A.
872 L. T. S. C. 2012. Loss of ATRX, genome instability, and an altered DNA damage
873 response are hallmarks of the alternative lengthening of telomeres pathway.
874 *PLoS Genet,* 8**,** e1002772.
875 MACIEJOWSKI, J. & DE LANGE, T. 2017. Telomeres in cancer: tumour suppression
876 and genome instability. *Nat Rev Mol Cell Biol,* 18**,** 175-186.
877 MAICHER, A., KASTNER, L., DEES, M. & LUKE, B. 2012. Deregulated telomere
878 transcription causes replication-dependent telomere shortening and promotes
879 cellular senescence. *Nucleic Acids Res,* 40**,** 6649-59.
880 MARION, R. M., MONTERO, J. J., LOPEZ DE SILANES, I., GRANA-CASTRO, O.,
881 MARTINEZ, P., SCHOEFTNER, S., PALACIOS-FABREGA, J. A. & BLASCO, M.
882 A. 2019. TERRA regulate the transcriptional landscape of pluripotent cells
883 through TRF1-dependent recruitment of PRC2. *Elife,* 8.
884 MCMURCHY, A. N., STEMPOR, P., GAARENSTROOM, T., WYSOLMERSKI, B.,
885 DONG, Y., AUSSIANIKAVA, D., APPERT, A., HUANG, N., KOLASINSKA-
886 ZWIERZ, P., SAPETSCHNIG, A., MISKA, E. A. & AHRINGER, J. 2017. A team
887 of heterochromatin factors collaborates with small RNA pathways to combat
888 repetitive elements and germline stress. *Elife,* 6.
889 MEIER, B., BARBER, L. J., LIU, Y., SHTESSEL, L., BOULTON, S. J., GARTNER, A. &
890 AHMED, S. 2009. The MRT-1 nuclease is required for DNA crosslink repair and
891 telomerase activity in vivo in Caenorhabditis elegans. *Embo J,* 28**,** 3549-63.

892 MEIER, B., CLEJAN, I., LIU, Y., LOWDEN, M., GARTNER, A., HODGKIN, J. &
893 AHMED, S. 2006. trt-1 is the Caenorhabditis elegans catalytic subunit of
894 telomerase. *PLoS Genet,* 2**,** e18.
895 MONTERO, J. J., LOPEZ-SILANES, I., MEGIAS, D., M, F. F., CASTELLS-GARCIA, A.
896 & BLASCO, M. A. 2018. TERRA recruitment of polycomb to telomeres is
897 essential for histone trymethylation marks at telomeric heterochromatin. *Nat*
898 *Commun,* 9**,** 1548.
899 MORAVEC, M., WISCHNEWSKI, H., BAH, A., HU, Y., LIU, N., LAFRANCHI, L., KING,
900 M. C. & AZZALIN, C. M. 2016. TERRA promotes telomerase-mediated telomere
901 elongation in Schizosaccharomyces pombe. *EMBO Rep,* 17**,** 999-1012.
902 ORTIZ, M. A., NOBLE, D., SOROKIN, E. P. & KIMBLE, J. 2014. A new dataset of
903 spermatogenic vs. oogenic transcriptomes in the nematode Caenorhabditis
904 elegans. *G3 (Bethesda),* 4**,** 1765-72.
905 PAK, J. & FIRE, A. 2007. Distinct populations of primary and secondary effectors during
906 RNAi in C. elegans. *Science,* 315**,** 241-4.
907 PANE, A., WEHR, K. & SCHUPBACH, T. 2007. zucchini and squash encode two
908 putative nucleases required for rasiRNA production in the Drosophila germline.
909 *Dev Cell,* 12**,** 851-62.
910 PARDUE, M. L. & DEBARYSHE, P. G. 2003. Retrotransposons provide an
911 evolutionarily robust non-telomerase mechanism to maintain telomeres. *Annu*
912 *Rev Genet,* 37**,** 485-511.
913 PERRINI, B., PIACENTINI, L., FANTI, L., ALTIERI, F., CHICHIARELLI, S., BERLOCO,
914 M., TURANO, C., FERRARO, A. & PIMPINELLI, S. 2004. HP1 controls telomere
915 capping, telomere elongation, and telomere silencing by two different
916 mechanisms in Drosophila. *Mol Cell,* 15**,** 467-76.
917 PFEIFFER, V. & LINGNER, J. 2012. TERRA promotes telomere shortening through
918 exonuclease 1-mediated resection of chromosome ends. *PLoS Genet,* 8**,**
919 e1002747.
920 PHILLIPS, C. M., MCDONALD, K. L. & DERNBURG, A. F. 2009. Cytological analysis of
921 meiosis in Caenorhabditis elegans. *Methods Mol Biol,* 558**,** 171-95.
922 PICKETT, H. A. & REDDEL, R. R. 2015. Molecular mechanisms of activity and
923 derepression of alternative lengthening of telomeres. *Nat Struct Mol Biol,* 22**,**
924 875-80.
925 POLO, S. E. & JACKSON, S. P. 2011. Dynamics of DNA damage response proteins at
926 DNA breaks: a focus on protein modifications. *Genes Dev,* 25**,** 409-33.
927 PORRO, A., FEUERHAHN, S., DELAFONTAINE, J., RIETHMAN, H., ROUGEMONT, J.
928 & LINGNER, J. 2014. Functional characterization of the TERRA transcriptome at
929 damaged telomeres. *Nat Commun,* 5**,** 5379.
930 QUINLAN, A. R. & HALL, I. M. 2010. BEDTools: a flexible suite of utilities for comparing
931 genomic features. *Bioinformatics,* 26**,** 841-2.
932 REINHART, B. J. & BARTEL, D. P. 2002. Small RNAs correspond to centromere
933 heterochromatic repeats. *Science,* 297**,** 1831.
934 ROAKE, C. M. & ARTANDI, S. E. 2017. Approaching TERRA Firma: Genomic
935 Functions of Telomeric Noncoding RNA. *Cell,* 170**,** 8-9.
936 ROSSIELLO, F., AGUADO, J., SEPE, S., IANNELLI, F., NGUYEN, Q., PITCHIAYA, S.,
937 CARNINCI, P. & D'ADDA DI FAGAGNA, F. 2017. DNA damage response

938 inhibition at dysfunctional telomeres by modulation of telomeric DNA damage
939 response RNAs. *Nat Commun,* 8**,** 13980.
940 SAGIE, S., TOUBIANA, S., HARTONO, S. R., KATZIR, H., TZUR-GILAT, A.,
941 HAVAZELET, S., FRANCASTEL, C., VELASCO, G., CHEDIN, F. & SELIG, S.
942 2017. Telomeres in ICF syndrome cells are vulnerable to DNA damage due to
943 elevated DNA:RNA hybrids. *Nat Commun,* 8**,** 14015.
944 SAKAGUCHI, A., SARKIES, P., SIMON, M., DOEBLEY, A. L., GOLDSTEIN, L. D.,
945 HEDGES, A., IKEGAMI, K., ALVARES, S. M., YANG, L., LAROCQUE, J. R.,
946 HALL, J., MISKA, E. A. & AHMED, S. 2014. Caenorhabditis elegans RSD-2 and
947 RSD-6 promote germ cell immortality by maintaining small interfering RNA
948 populations. *Proc Natl Acad Sci U S A,* 111**,** E4323-31.
949 SARIN, K. Y., CHEUNG, P., GILISON, D., LEE, E., TENNEN, R. I., WANG, E.,
950 ARTANDI, M. K., ORO, A. E. & ARTANDI, S. E. 2005. Conditional telomerase
951 induction causes proliferation of hair follicle stem cells. *Nature,* 436**,** 1048-52.
952 SAVITSKY, M., KWON, D., GEORGIEV, P., KALMYKOVA, A. & GVOZDEV, V. 2006.
953 Telomere elongation is under the control of the RNAi-based mechanism in the
954 Drosophila germline. *Genes Dev,* 20**,** 345-54.
955 SCHAETZLEIN, S., KODANDARAMIREDDY, N. R., JU, Z., LECHEL, A.,
956 STEPCZYNSKA, A., LILLI, D. R., CLARK, A. B., RUDOLPH, C., KUHNEL, F.,
957 WEI, K., SCHLEGELBERGER, B., SCHIRMACHER, P., KUNKEL, T. A.,
958 GREENBERG, R. A., EDELMANN, W. & RUDOLPH, K. L. 2007. Exonuclease-1
959 deletion impairs DNA damage signaling and prolongs lifespan of telomere-
960 dysfunctional mice. *Cell,* 130**,** 863-77.
961 SHAY, J. W. 2016. Role of Telomeres and Telomerase in Aging and Cancer. *Cancer*
962 *Discov,* 6**,** 584-93.
963 SHIMAMOTO, A., YOKOTE, K. & TAHARA, H. 2015. Werner Syndrome-specific
964 induced pluripotent stem cells: recovery of telomere function by reprogramming.
965 *Front Genet,* 6**,** 10.
966 SHIRAYAMA, M., STANNEY, W., 3RD, GU, W., SETH, M. & MELLO, C. C. 2014. The
967 Vasa Homolog RDE-12 engages target mRNA and multiple argonaute proteins to
968 promote RNAi in C. elegans. *Curr Biol,* 24**,** 845-51.
969 STEINER, F. A., OKIHARA, K. L., HOOGSTRATE, S. W., SIJEN, T. & KETTING, R. F.
970 2009. RDE-1 slicer activity is required only for passenger-strand cleavage during
971 RNAi in Caenorhabditis elegans. *Nat Struct Mol Biol,* 16**,** 207-11.
972 TABARA, H., YIGIT, E., SIOMI, H. & MELLO, C. C. 2002. The dsRNA binding protein
973 RDE-4 interacts with RDE-1, DCR-1, and a DExH-box helicase to direct RNAi in
974 C. elegans. *Cell,* 109**,** 861-71.
975 TAYLOR, D. H., CHU, E. T., SPEKTOR, R. & SOLOWAY, P. D. 2015. Long non-coding
976 RNA regulation of reproduction and development. *Mol Reprod Dev,* 82**,** 932-56.
977 TEAM, R. C. 2017. R: A language and environment for statistical computing. R
978 Foundation for Statistical Computing, Vienna, Austria. https://www.R-project.org/.
979 TIJSTERMAN, M., KETTING, R. F., OKIHARA, K. L., SIJEN, T. & PLASTERK, R. H.
980 2002. RNA helicase MUT-14-dependent gene silencing triggered in C. elegans
981 by short antisense RNAs. *Science,* 295**,** 694-7.
982 TOUBIANA, S. & SELIG, S. 2018. DNA:RNA hybrids at telomeres - when it is better to
983 be out of the (R) loop. *FEBS J,* 285**,** 2552-2566.

UDUGAMA, M., FT, M. C., CHAN, F. L., TANG, M. C., PICKETT, H. A., JD, R. M., MAYNE, L., COLLAS, P., MANN, J. R. & WONG, L. H. 2015. Histone variant H3.3 provides the heterochromatic H3 lysine 9 tri-methylation mark at telomeres. *Nucleic Acids Res,* 43**,** 10227-37.

VRBSKY, J., AKIMCHEVA, S., WATSON, J. M., TURNER, T. L., DAXINGER, L., VYSKOT, B., AUFSATZ, W. & RIHA, K. 2010. siRNA-mediated methylation of Arabidopsis telomeres. *PLoS Genet,* 6**,** e1000986.

WANAT, J. J., LOGSDON, G. A., DRISKILL, J. H., DENG, Z., LIEBERMAN, P. M. & JOHNSON, F. B. 2018. TERRA and the histone methyltransferase Dot1 cooperate to regulate senescence in budding yeast. *PLoS One,* 13**,** e0195698.

WEDELES, C. J., WU, M. Z. & CLAYCOMB, J. M. 2013. Protection of germline gene expression by the C. elegans Argonaute CSR-1. *Dev Cell,* 27**,** 664-71.

WELKER, N. C., PAVELEC, D. M., NIX, D. A., DUCHAINE, T. F., KENNEDY, S. & BASS, B. L. 2010. Dicer's helicase domain is required for accumulation of some, but not all, C. elegans endogenous siRNAs. *RNA,* 16**,** 893-903.

WICKY, C., VILLENEUVE, A. M., LAUPER, N., CODOUREY, L., TOBLER, H. & MULLER, F. 1996. Telomeric repeats (TTAGGC)n are sufficient for chromosome capping function in Caenorhabditis elegans. *Proc Natl Acad Sci U S A,* 93**,** 8983-8.

WONG, L. H., MCGHIE, J. D., SIM, M., ANDERSON, M. A., AHN, S., HANNAN, R. D., GEORGE, A. J., MORGAN, K. A., MANN, J. R. & CHOO, K. H. 2010. ATRX interacts with H3.3 in maintaining telomere structural integrity in pluripotent embryonic stem cells. *Genome Res,* 20**,** 351-60.

ZELLER, P., PADEKEN, J., VAN SCHENDEL, R., KALCK, V., TIJSTERMAN, M. & GASSER, S. M. 2016. Histone H3K9 methylation is dispensable for Caenorhabditis elegans development but suppresses RNA:DNA hybrid-associated repeat instability. *Nat Genet,* 48**,** 1385-1395.

ZHANG, W., LI, J., SUZUKI, K., QU, J., WANG, P., ZHOU, J., LIU, X., REN, R., XU, X., OCAMPO, A., YUAN, T., YANG, J., LI, Y., SHI, L., GUAN, D., PAN, H., DUAN, S., DING, Z., LI, M., YI, F., BAI, R., WANG, Y., CHEN, C., YANG, F., LI, X., WANG, Z., AIZAWA, E., GOEBL, A., SOLIGALLA, R. D., REDDY, P., ESTEBAN, C. R., TANG, F., LIU, G. H. & BELMONTE, J. C. 2015. Aging stem cells. A Werner syndrome stem cell model unveils heterochromatin alterations as a driver of human aging. *Science,* 348**,** 1160-3.

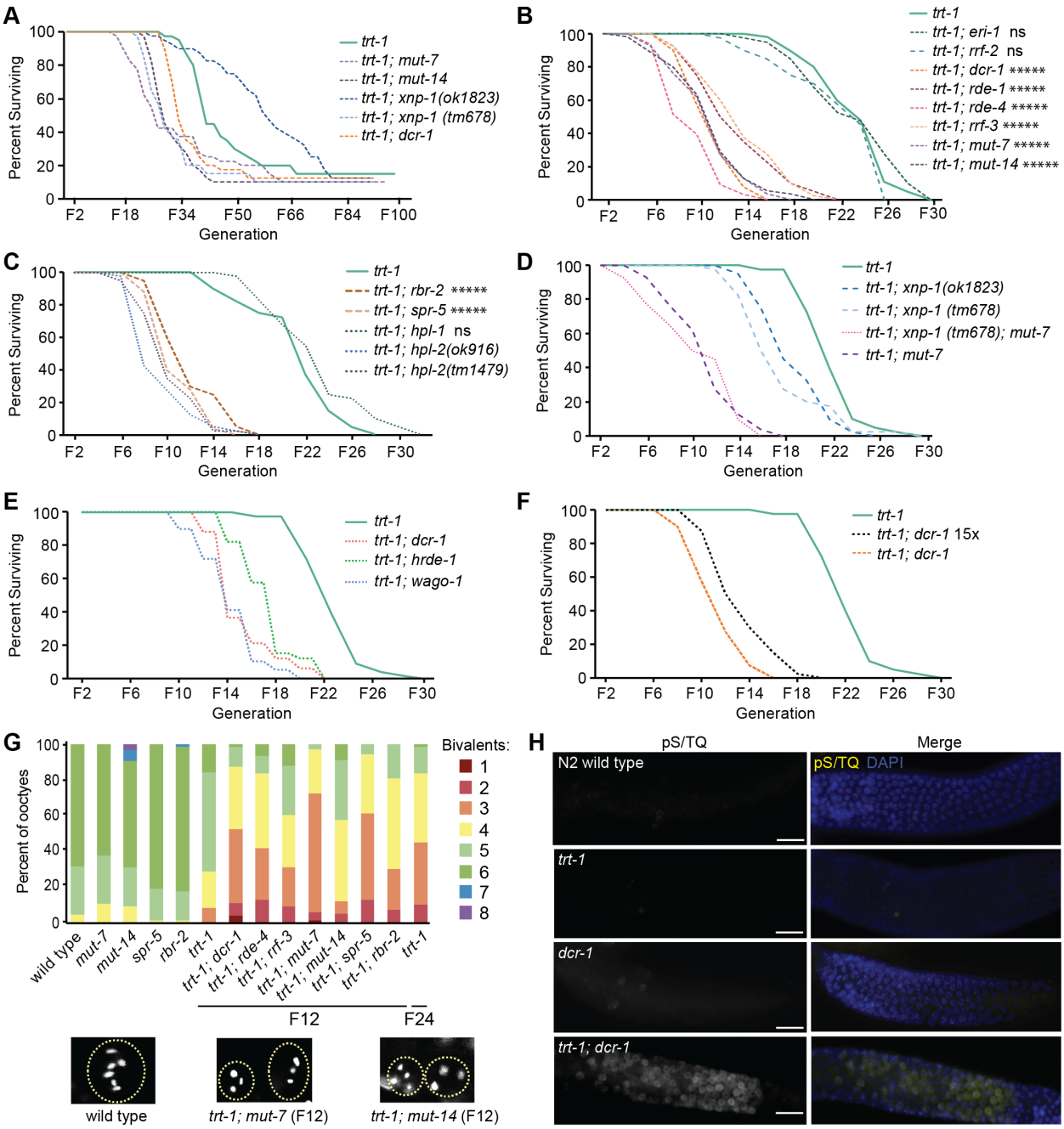

Figure 1: Endogenous small RNA and chromatin factors repress telomere stability in the absence of telomerase. (A) Survival curve of telomerase-deficient strains passaged at ~100 worms weekly for 40 independent lines. One allele of *xnp-1(ok1823)* extended survival but did not increase survival via ALT (Table S1). The same wild type control data is shown in panels B-F. (B) Survival curve of primary or secondary sRNA deficient telomerase mutants when 6 larval L1s are passaged weekly. (C) Survival curve of double mutants for *trt-1* and chromatin factors passaged by 6 L1s weekly. (D) Histone H3.3 remodeling protein XNP-1 represses senescence in *trt-1* mutants epistatically to the small RNA factor MUT-7. (E) Loss of HRDE-1 or WAGO-1 Argonaute proteins mimics the accelerated sterility observed in a *trt-1; dcr-1* mutant background. (F) A *trt-*

1034 *1; dcr-1* strain was crossed with *dcr-1* males fifteen times to yield a *trt-1; dcr-1* 15x strain
1035 that displayed the same accelerated sterility observed for the initial *trt-1; dcr-1* double
1036 mutants. (G) Small RNA and heterochromatin mutant *trt-1* lines have high levels of
1037 chromosome fusions, comparable to *trt-1* single mutants at F24. Fusions were assayed
1038 by diamidino-2-phenylindole (DAPI) staining of oocytes in diakinesis. Each bivalent in
1039 wildtype represents a single paired chromosome. Representative images of DAPI-
1040 stained oocyte nuclei are shown in panels below the graph. (H) High levels of phospho-
1041 (Ser/Thr) staining in the meiotic gonad of *trt-1; dcr-1* at F6 compared to N2 or *trt-1*.
1042 Scale bar, 25□m. (B)-(D), (F) ***$p < 0.001$; ****$p < 0.00001$; ns, not significant, (Log
1043 rank test, n=40 independent lines for each genotype). (E) *trt-1; wago-1* = 39 lines per
1044 genotype. *trt-1; hrde-1* and *trt-1; dcr-1* = 33 lines per genotype.
1045

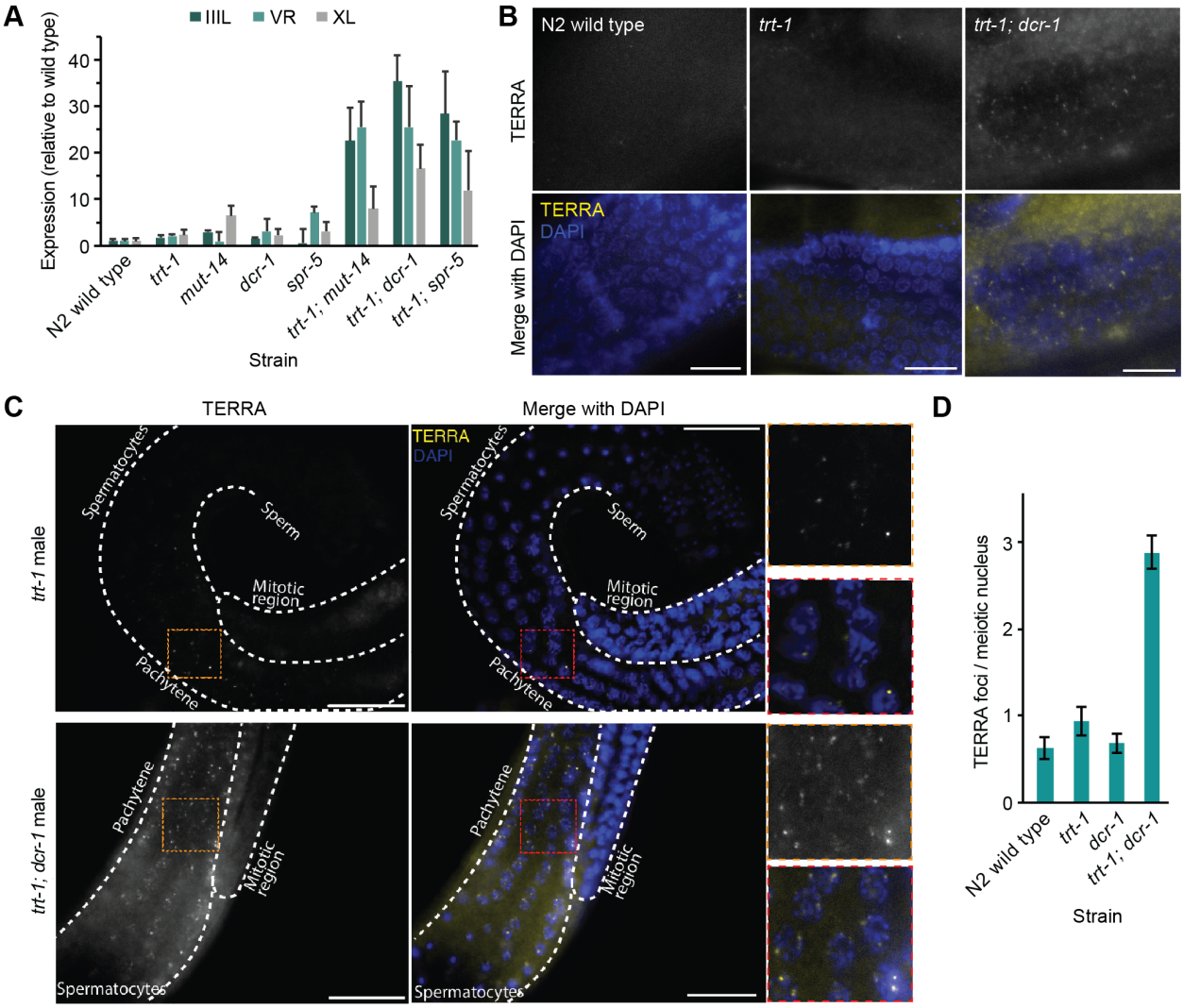

Figure 2: (A) Expression of TERRA from subtelomeres *IIIL*, *VR*, and *XL* is increased in sRNA and heterochromatin deficient telomerase mutants. cDNA was reverse transcribed with a telomere specific primer and qPCR was performed using subtelomere-specific primer pairs and normalized to *act-1*. Expression data are plotted relative to wildtype and represent the mean ± SEM of three biological replicates. (B) RNA FISH signals of TERRA in meiotic germlines of hermaphrodites of the indicated genotypes. TERRA foci are present in wildtype and *trt-1* in the pachytene region and increased in *trt-1; dcr-1.* Scale bar, 10um. (C) Representative RNA FISH images of TERRA in males show foci in the pachytene region of the germline which are increased in *trt-1; dcr-1* compared to *trt-1.* Scale bar, 20 um. (D) Quantification of germline TERRA foci (mean ± SEM, n=10 germlines).

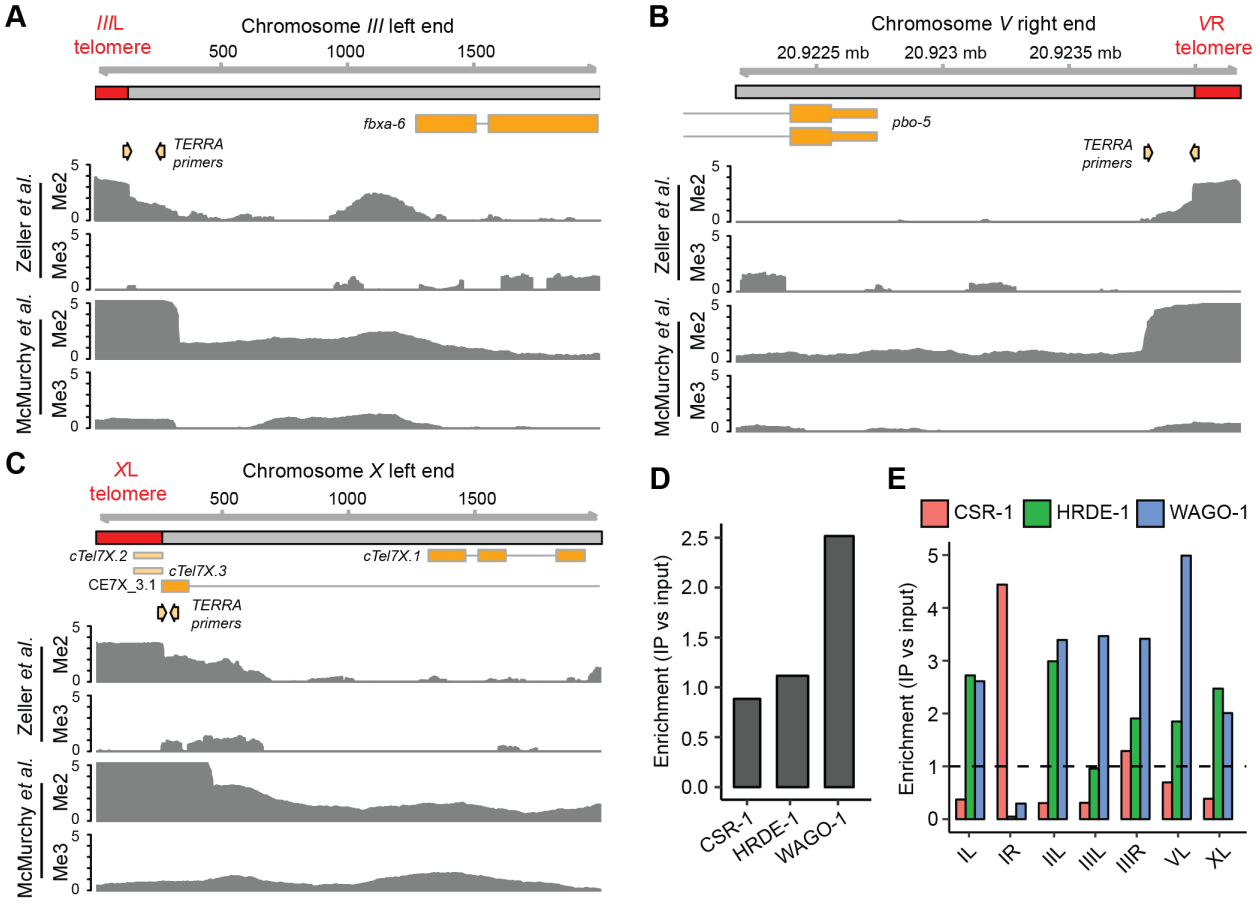

Figure 3: Analysis of telomeric chromatin and small RNAs in published datasets. (A)-(C) ChIP-seq enrichment profiles at three chromosome ends constructed using published data (McMurchy et al., 2017, Zeller et al., 2016). Small orange arrows between gene models and data tracks show the position of primers used in TERRA qRT-PCR experiments. (D) Enrichment (IP/input) of reads mapping to perfect telomere sequence with up to three mismatches in published immunoprecipitation datasets for three different Argonaute proteins. (E) Enrichment for subtelomeric sRNAs for datasets used in (D).

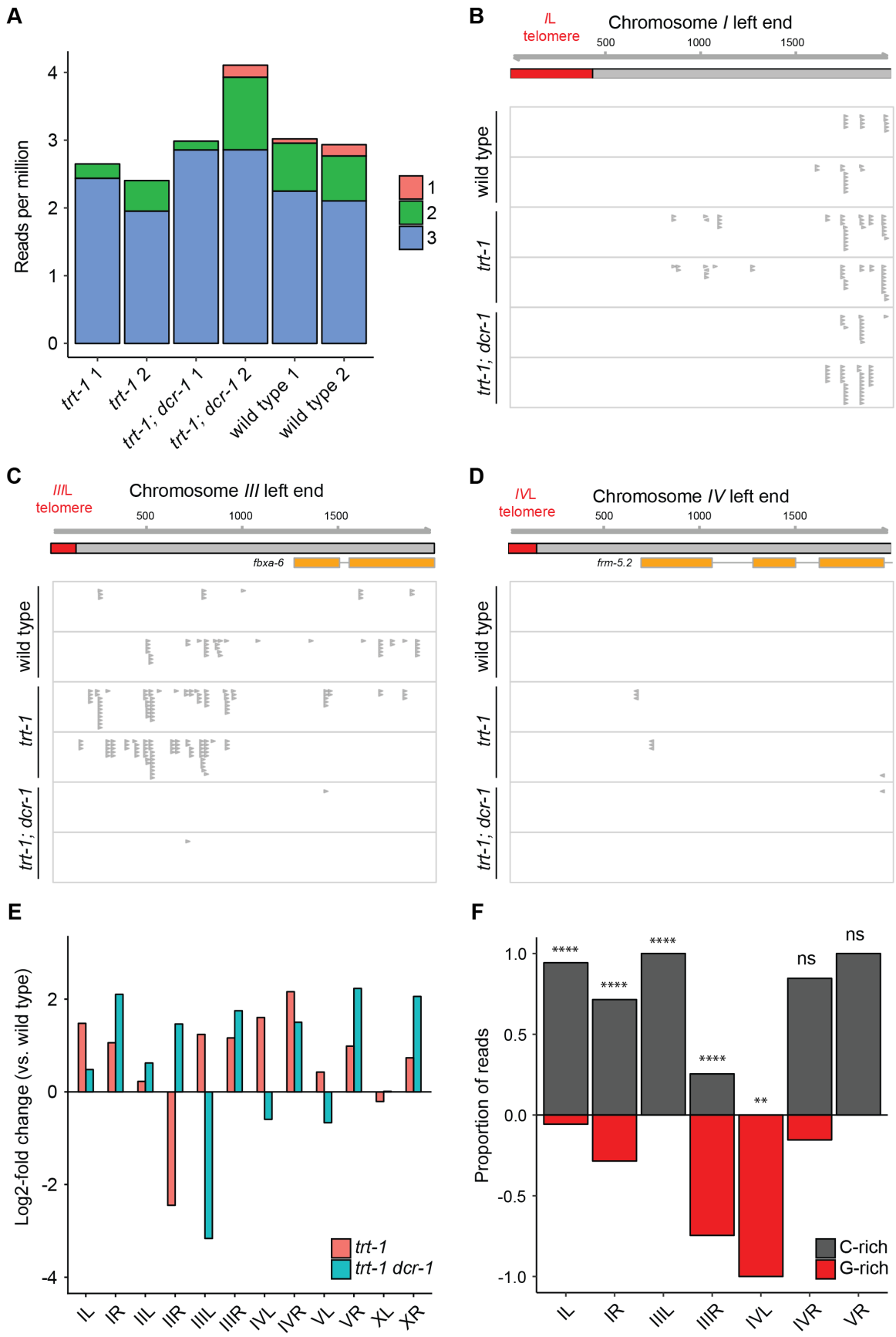
A
Reads per million
0
1
2
3
4
trt-1 1
trt-1 2
trt-1; dcr-1 1
trt-1; dcr-1 2
wild type 1
wild type 2
1
2
3
B
IL telomere
Chromosome I left end
500
1000
1500
wild type
trt-1
trt-1; dcr-1
C
IIIL telomere
Chromosome III left end
500
1000
1500
fbxa-6
wild type
trt-1
trt-1; dcr-1
D
IVL telomere
Chromosome IV left end
500
1000
1500
frm-5.2
wild type
trt-1
trt-1; dcr-1
E
Log2-fold change (vs. wild type)
-4
-2
0
2
trt-1
trt-1 dcr-1
IL
IR
IIL
IIR
IIIL
IIIR
IVL
IVR
VL
VR
XL
XR
F
Proportion of reads
1.0
0.5
0.0
-0.5
-1.0
****
****
****
****
**
ns
ns
C-rich
G-rich
IL
IR
IIIL
IIIR
IVL
IVR
VR

1071

1072
1073 **Figure 4:** Upregulation of subtelomeric sRNAs in telomerase mutants. (A) Number of
1074 telomere-mapping reads in wild-type, *trt-1,* and *trt-1;dcr-1* libraries. Numbers 1-3
1075 indicate number of mismatches. (B)-(D) 22G sRNAs at three subtelomeres. (E) Log2-
1076 fold change in sRNA abundance at subtelomeres relative to wildtype in *trt-1* and *trt-1;*
1077 *dcr-1* animals. (F) Proportion of subtelomeric sRNAs mapping to the strand
1078 corresponding to the G-rich (TTAGGC) and C-rich (TAAGCC) telomere strand in *trt-1*
1079 animals. **** $p < 0.0001$; ** $p < 0.01$; ns, not significant (Binomial test with Bonferroni
1080 correction). The p values refer to the probability of observing the given proportion of G-rich
1081 or C-rich telomeric reads at each chromosome end under the null hypothesis that G- and
1082 C-rich reads are present in equal proportions.
1083

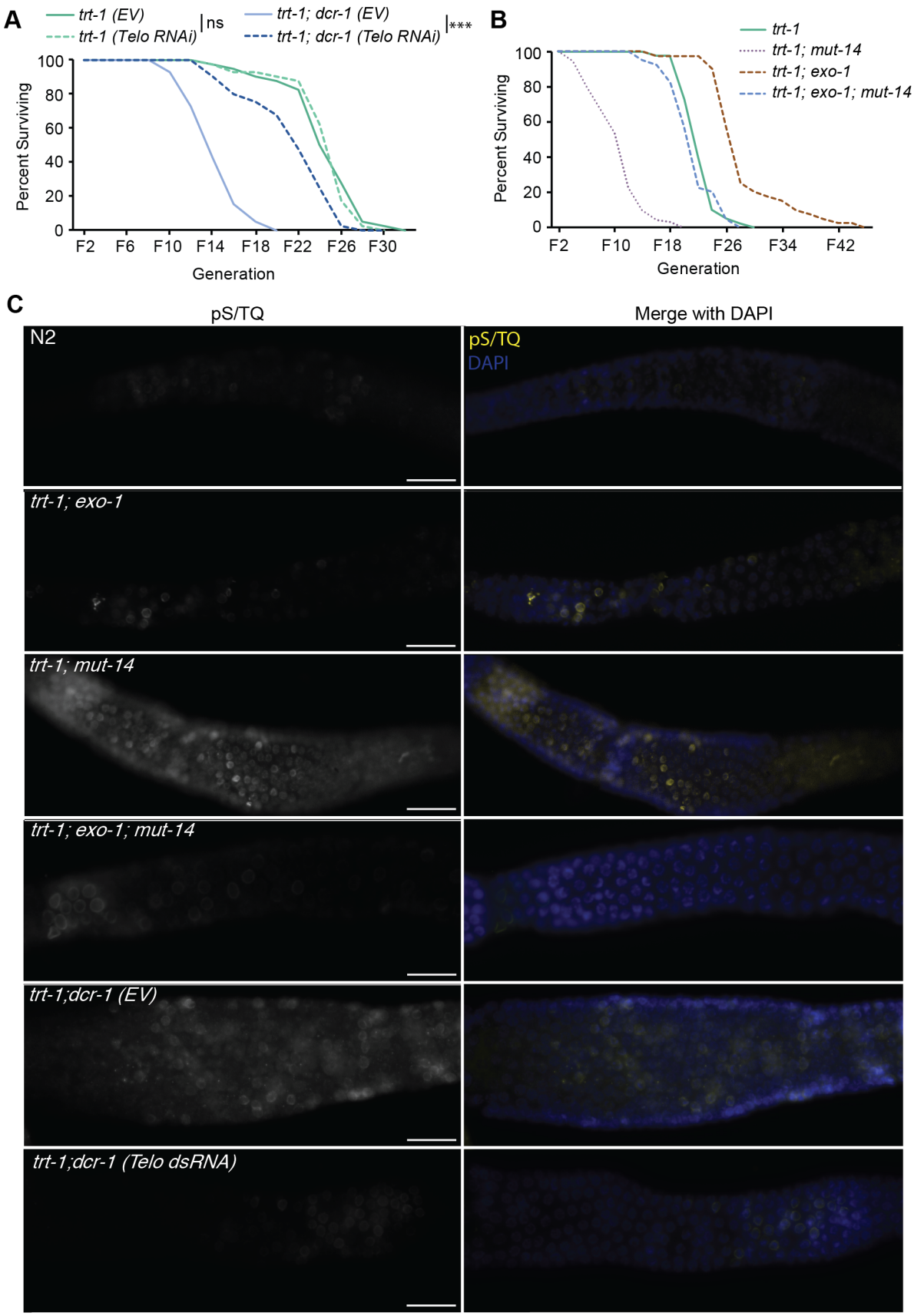
A
trt-1 (EV)
trt-1 (Telo RNAi)
ns
trt-1; dcr-1 (EV)
trt-1; dcr-1 (Telo RNAi)
***
Percent Surviving
100
80
60
40
20
0
F2
F6
F10
F14
F18
F22
F26
F30
Generation
B
trt-1
trt-1; mut-14
trt-1; exo-1
trt-1; exo-1; mut-14
Percent Surviving
100
80
60
40
20
0
F2
F10
F18
F26
F34
F42
Generation
C
pS/TQ
Merge with DAPI
N2
pS/TQ
DAPI
trt-1; exo-1
trt-1; mut-14
trt-1; exo-1; mut-14
trt-1;dcr-1 (EV)
trt-1;dcr-1 (Telo dsRNA)

1084

1085
1086 **Figure 5:** Fast senescence in sRNA-deficient *trt-1* is rescued by exogenous telomeric
1087 dsRNA or loss of Exonuclease-1. (A) Survival of *trt-1* or *trt-1; dcr-1(mg375)* on either
1088 empty vector control (EV) or bacteria expressing telomeric double-stranded RNA (telo
1089 dsRNA). Log rank test relative to EV, ***P < 0.001. n=40 lines per genotype. (B) Loss
1090 of *exo-1* extends survival of *trt-1; mut-14* lines. n=40 lines per genotype. (C) Telomeric
1091 dsRNA and loss of *exo-1* suppress accumulation of phospho-(Ser/Thr) in sRNA-
1092 deficient *trt-1* by F6. Scale bar=20um.
1093
1094
1095

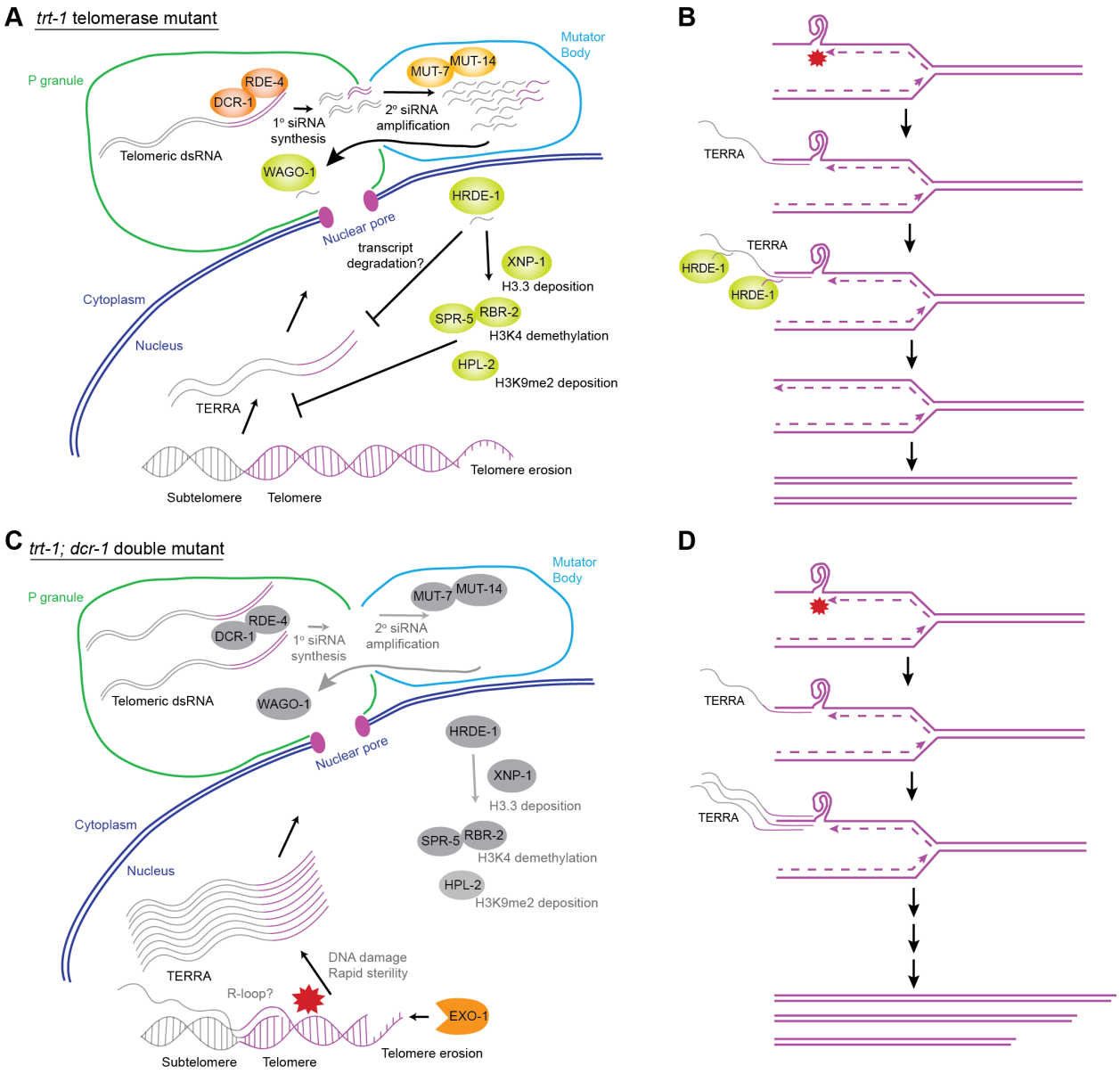

Figure 6: Model for TERRA, small RNAs and telomerase. A) In *trt-1* telomerase mutants, telomeric erosion induces expression of the lncRNA TERRA, which engages production of sub-telomeric and telomeric sRNAs. Small RNAs promote deposition of H3K9me2 and H3K4 demethylation in order to repress TERRA expression DNA damage, and *trt-1* mutant sterility. B) TERRA expression and silencing may occur in the context of a DNA damage response. C) In *trt-1; dcr-1* double mutants, TERRA expression is not repressed, which may cause RNA:DNA hybrids and a form of recombination that is dependent on the nuclease EXO-1 and leads to rapid sterility. D) Lack of sRNAs may induce an aberrant recombinational response to DNA damage that results in telomere elongation or shortening.

Supplemental Information

5 Supplemental Figures

3 Supplemental Tables

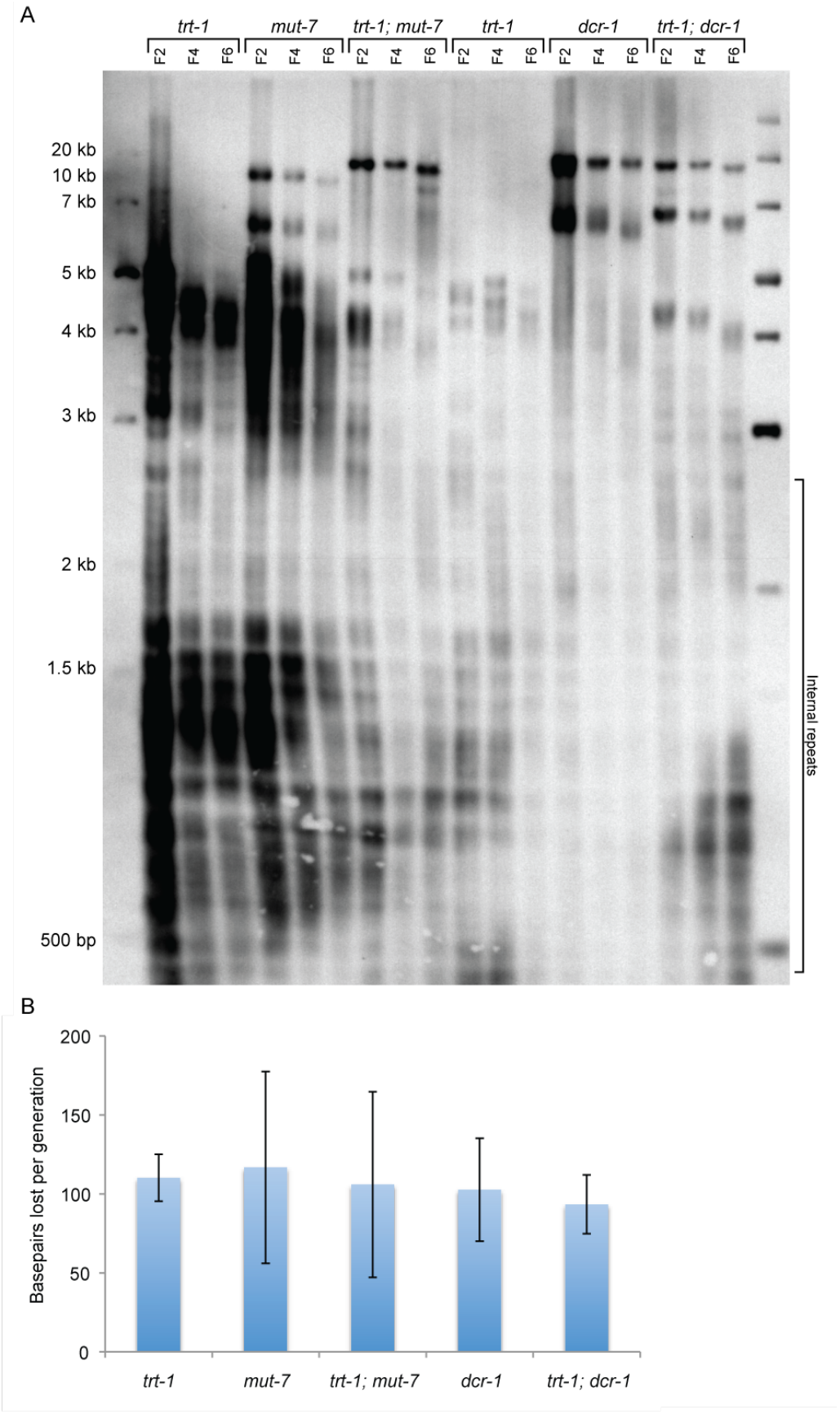
A
trt-1
mut-7
trt-1; mut-7
trt-1
dcr-1
trt-1; dcr-1
F2
F4
F6
20 kb
10 kb
7 kb
5 kb
4 kb
3 kb
2 kb
1.5 kb
500 bp
Internal repeats
B
Basepairs lost per generation
200
150
100
50
0
trt-1
mut-7
trt-1; mut-7
dcr-1
trt-1; dcr-1

1118

1119 **Figure S1. Related to Figure 1.** Terminal Restriction Fragment (TFR) analysis of
1120 single-mutant *trt-1*, *mut-7*, and *dcr-1* and double-mutant *trt-1; mut-7* and *trt-1; dcr-1*
1121 strains using a telomeric probe. (A) Southern blot of samples generated by passaging
1122 small groups of worms for multiple generations. Two independent *trt-1* lines were used.
1123 Long telomeres observed in strains derived from *mut-7* or *dcr-1* mutant background
1124 could be due to rare stochastic telomere elongation events in these backgrounds. (B)
1125 Quantification of telomere shortening rate for each genotype shown in panel A. No
1126 significant difference was found between any genotypes by Mann Whitney U test.
1127
1128

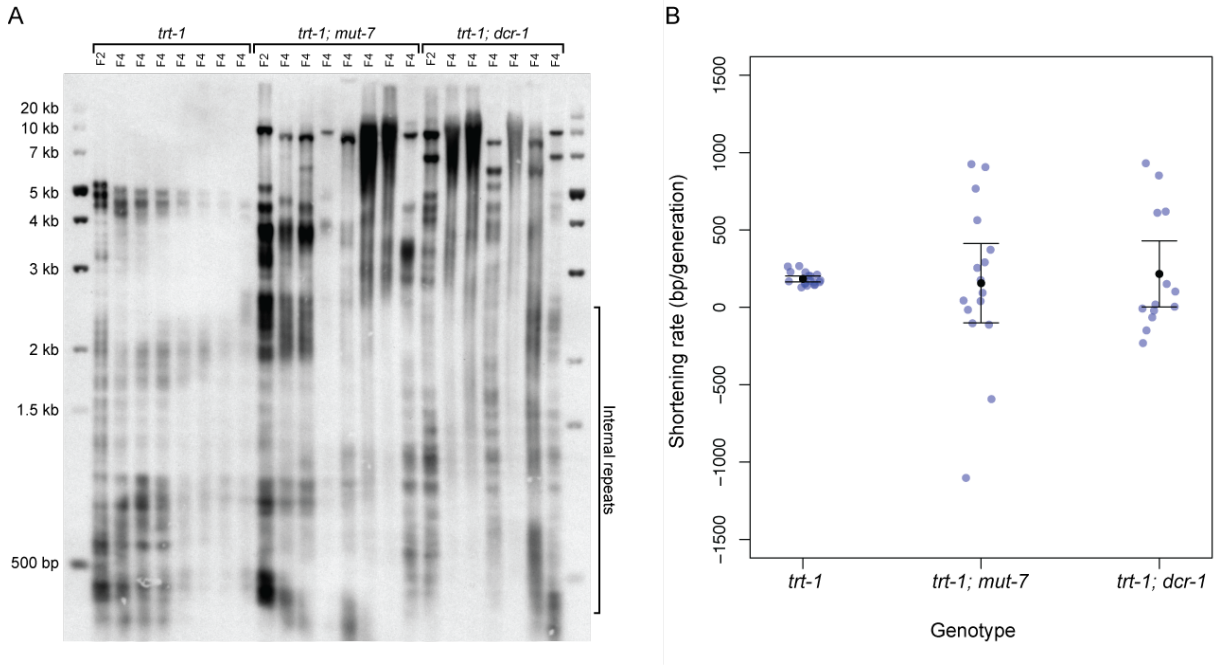

Figure S2. Related to Figure 1. TRF analysis of RNAi-deficient telomerase mutant strains using telomeric probe. A) A single parental F2 plate was used to generate multiple F4 plates derived from single worms. F4 *trt-1* single mutant lanes show consistent bands corresponding to slight shortening of parental bands. In contrast, F4 lanes from *trt-1; mut-7* and *trt-1; dcr-1* show highly variable bands that in some cases cannot be traced to an obvious parental band. B) Quantification of telomere shortening rate based on pairing bands appearing at F2 with the closest bands appearing at F4. Highly smeared lanes were excluded. Each point represents one pair of bands. Comparing *trt-1* and *trt-1; mut-7* or *trt-1; dcr-1*, mean shortening rate was not significantly different (p= 0.84 and 0.77, Welch's t-test) but variance was significantly higher for both double-mutants (p=7.2e-15 and 1.5e-12, F-test). Variance was not significantly different between the double-mutants (p=0.32).

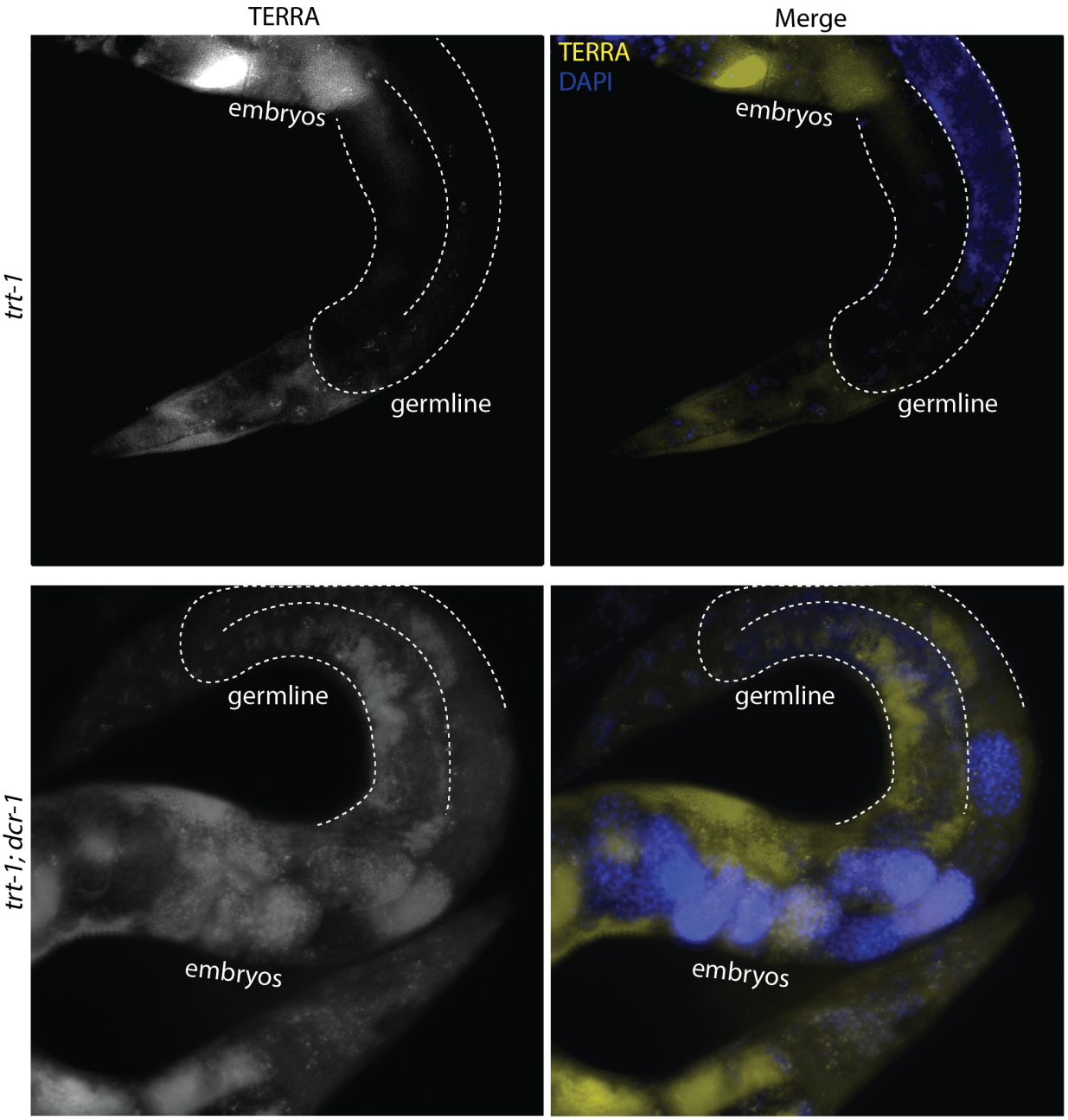

1144

1145 **Figure S3. Related to Figure 2.** TERRA expression (yellow) in *trt-1* and *trt-1; dcr-*
1146 *1(mg375)* 1-day-old adults detected with a Cy5-labelled telomeric probe.

1147
1148
1149

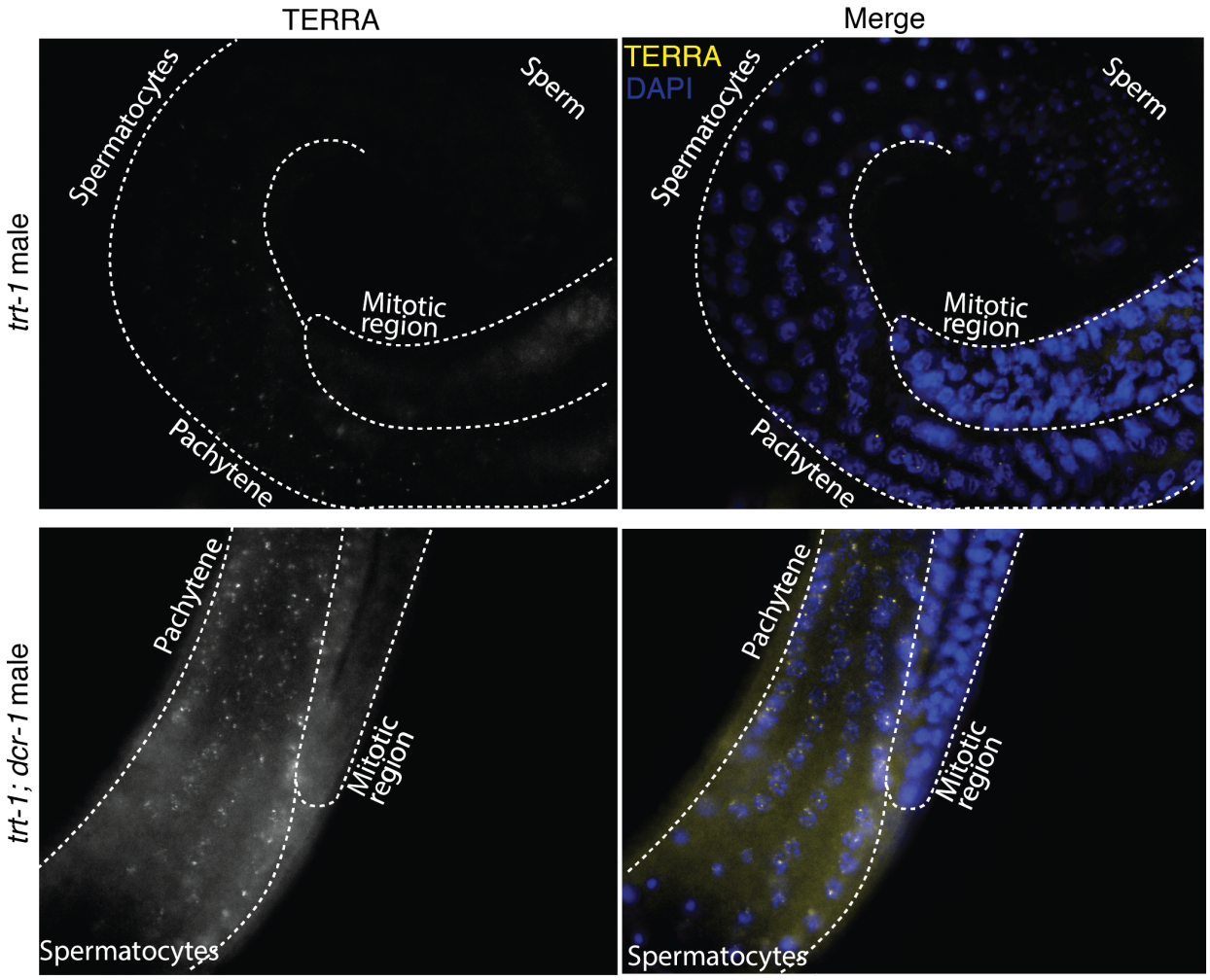

Figure S4. Related to Figure 2. RNA FISH of TERRA expression in *trt-1* and *trt-1; dcr-1* males. Note TERRA foci in the Pachytene region in both *trt-1* and *trt-1; dcr-1*, as well as lack of expression in the mitotic region and spermatocytes

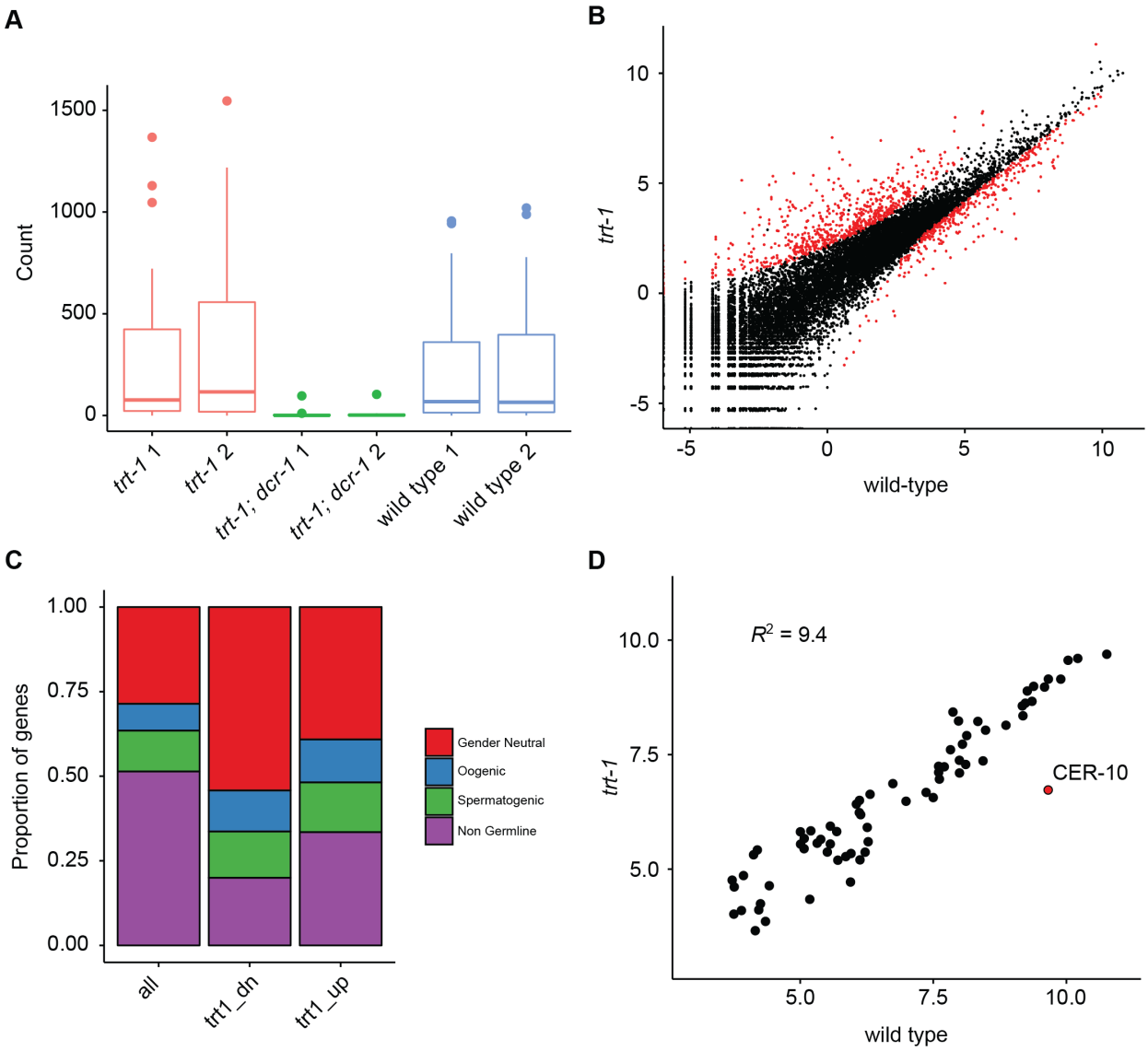

Figure S5. Related to Figure 3. Analysis of 22G small RNA species in telomerase and Dicer mutants. (A) Number of reads mapping to DCR-1 targets identified by Gent *et al.* (Gent et al., 2010). (B) log2 normalized mean read counts at every *C. elegans* gene for *trt-1* and wildtype. Genes identified as significantly differentially expressed by DESeq2 are shown in red. (C) Proportion of all genes or genes downregulated (trt1_dn) or upregulated (trt1_up) belonging to expression categories defined by Ortiz *et al.* (see reference 54 in main text). (D) log2 normalized mean read counts at transposon consensus sequences for *trt-1* and wildtype.

	Lines tested	Number ALT survivors	Z score	p-value (two tailed)
trt-1	40	6		
trt-1; mut-7(pk204)	40	4	0.68	0.50
trt-1; mut-14(pk738)	40	4	0.68	0.50
trt-1 xnp-1(ok1823)	40	6	0	1
trt-1 xnp-1(tm678)	40	4	0.68	0.50
trt-1; dcr-1 (mg375)	40	5	0.32	0.75

Supplemental Table S1. Related to Figure 1. Statistical analysis of ALT survival in double mutant strains compared to single mutant *trt-1* control. The Z score represents how many standard deviations from the number of ALT survivors in double mutants is from the *trt-1* single mutant control mean survival rate. The p-value represents the probability that the number of survivors via ALT is not significantly different from the control *trt-1* single mutant strain.

1201
1202

Strain	Log Rank test (Z=)	p-value
trt-1; mut-7(pk204)	9.79	<0.00001
trt-1; mut-14(pk738)	9.96	<0.00001
trt-1; dcr-1(mg375)	9.37	<0.00001
trt-1; rde-1	8.23	<0.00001
trt-1; rde-4	9.21	<0.00001
trt-1; rrf-3	8.4	<0.00001
trt-1; rrf-2	1.7	0.089
trt-1; exo-1	7.38	<0.00001
trt-1 xnp-1(ok1823)	4.3	<0.00001
trt-1 xnp-1(tm678)	4.23	<0.0001
trt-1 xnp-1(tm678); mut-7	9.21	<0.00001
trt-1; sid-1	6.52	<0.00001
trt-1; rbr-2(tm1231)	8.64	<0.00001
trt-1; spr-5 (by101)	8.89	<0.00001

Supplemental Table S2. Related to Figure 1. Log rank analysis of survival curves of double or triple mutants compare to single mutant *trt-1* controls. n=40 independent lines for each genotype. Strains were passaged by transferring 6 larval L1s weekly and scored as sterile when plates contained no new L1 larvae. The p-value represents the probability that there is no difference in the probability of sterility at any time point between the double or triple mutant strain and the *trt-1* single mutant strain.

trt-1 F1	males	dead embryos	*trt-1; dcr-1* F1	males	dead embryos
A1	13	6	A1	0	0
A2	4	26	A2	0	0
A3	8	24	A3	1	0
D1	10	11	A4	0	0
D2	11	4	B1	0	0
D3	4	9	B2	0	0
D4	13	15	B3	0	0
			B4	0	0
			C1	0	0
			C2	0	6
			C3	1	0
			C4	0	0
			D1	0	0
			D2	0	0
			D3	0	0
			D4	0	0

Supplemental Table S3. Related to Figure 1. Counts of total F2 males and dead embryos scored for F1 progeny from crosses of wild-type males with either late-generation F16 *trt-1* mutant controls (n=2 independently grown strains, three F1 scored for strain A and four F1 for strain D) or early generation F4 *trt-1; dcr-1* double mutant (n=4 strains, 4 F1 each scored for strains A, B, C, and D) hermaphrodites. If a chromosome fusion is present in any of the F1 animals, then it will cause weak non-disjunction of the fused chromosomes, which leads to F2 dead embryos if an autosome is fused or to F2 males if the X chromosome is fused.